NAGOYA UNIVERSITY

The Wear Effect of Molybdenum-derived Particles on The Hydrogenated Diamond-like Carbon under Boundary Lubrication

Khairul Amzar Bin Mohd Kassim

A thesis submitted in partial fulfillment for the degree of

Doctor of Engineering

in the

DEPARTMENT OF MICRO-NANO

MECHANICAL SCIENCE AND ENGINEERING

GRADUATE SCHOOL OF ENGINEERING

2023

NAGOYA UNIVERSITY

Abstract

DEPARTMENT OF MICRO-NANO MECHANICAL SCIENCE & ENGINEERING

GRADUATE SCHOOL OF ENGINEERING

Doctor of Engineering

by Khairul Amzar Bin Mohd Kassim

In the modern world, a massive amount of energy has been lost from the automobile sector caused by the poor performance of mechanical parts, especially inside the automobile engine. A lot of advanced technologies have been explored to counter this problem and one of them is diamond-like carbon (DLC). DLC has desirable mechanical and chemical properties for coating industries since it has superior properties such as low friction and wear, high hardness, and high chemical stability.

In most applications inside the automobile engine, DLC coatings always work together with lubricants and additives in order to improve the efficiency, durability, and sustainability of the engine. Usually, 10% of additives are added to a lubricant to enhance its lubricating capabilities under lubrication regimes. This mixture includes friction modifiers, anti-wear, antioxidants, viscosity improvers, detergents, corrosion inhibitors, emulsifiers, and extreme pressure additives. However, some of these additives affect the functionality of DLC.

The study on the tribological behaviour of additives toward DLC coating has

captured the attention of many researchers. Molybdenum dithiocarbamate (MoDTC), a well-known friction-modifier additive was reported to be degradable into other materials and has wear accelerating effects on DLC/steel sliding contact. However, the effect of each material and which compound mainly accelerates the wear of DLC has not been clarified yet. Further studies about this phenomenon are very essential to get a better understanding of the wear effects as it is quite critical especially in automotive components as the wear will shorten the lifetime of DLC and disturbs the engine performance.

In this present study, the first objective is to identify and classify the role of Mo-derived compounds that enhances wear under boundary lubrication at room temperature. Powder-type MoDTC, MoO_3, Mo_2C, MoS_2, and Mo were dispersed into Poly-alpha-olefin (PAO) base oil with a 0.1% volume percentage. The particle sizes are between 2.0-5.0 μm and the mixtures were tribologically tested on two types of DLC, a-C:H and Si-DLC against a steel ball at 23°C. The friction and wear, FESEM, and Raman observation results of each particle were carefully analyzed.

For friction of a-C:H, MoO_3 showed the most effective particle to increase the friction coefficient to approximately 0.17. MoDTC and MoS_2 showed almost the same lowest value at approximately 0.10. On the other hand, Mo_2C and Mo indicated a friction coefficient of nearly 0.12 and 0.14, respectively. Meanwhile, for Si-DLC, Mo contributed to the highest friction coefficient about 0.13, and MoDTC had an effect of the utmost friction reduction approximately at 0.09. Mo_2C showed a moderate friction coefficient at around 0.12 after the running-in period until the end of sliding cycles.

Meanwhile, the specific wear rate of MoDTC showed a high value, approximately 3.2×10^{-6} mm^3/Nm for a-C:H and 1.5×10^{-6} mm^3/Nm for Si-DLC.

However, Mo_2C had 10 times higher specific wear rate compared to MoDTC for both DLC. MoO_3 showed a higher specific wear rate approximately 1.1 x 10^{-6} mm^3/Nm, but still much lower compared to MoDTC for both discs. MoS_2 and Mo maintained their lowest specific ware rate values for both a-C:H and Si-DLC.

FESEM and Raman observations determine the wear type of the Mo-derived particles. If there is an increment of the I_D/I_G ratio, it indicates that graphitization and structural changes took place. Based on the investigation, it can be concluded that MoO_3 gives a catalytic effect to accelerate wear. On the other hand, MoDTC might have a role to accelerate wear by chemical assistance regardless of its hardness. Mo_2C from MoDTC degradation was the major contributor as it accelerates wear abrasively. The results for MoS_2 and Mo were not severe as they are solid lubricants that formed a protective layer and cover the asperities between DLC/steel surfaces.

After the wear classification has been completed at room temperature, the next objective is to continue the further investigation in standard operating engine temperature with a mixing effect. For this experiment, only a-C:H DLC was tested. The same procedures took place, MoDTC, MoS_2, Mo, MoO_3, and Mo_2C additives particles were dispersed individually into a base oil and tested on an a-C:H sliding against a steel ball under boundary lubrication at 80ºC.

At this stage, the application of surface-enhanced Raman scattering (SERS) was scrutinized. SERS measurements provide more accurate results compared to normal Raman analysis. SERS analysis only included at most 2 nm below the topmost surface. Meanwhile, normal Raman wavelength can penetrate through the coating surface to depths of several hundred nanometers to micrometers. The final result is affected by the deeper layers and is not accurate. Thus, SERS analysis is the best option to investigate

the actual condition that happened on the topmost surface of DLC.

SERS measurement implied the value of hydrogen content. It can be calculated by using a formula. From investigation, MoS_2 showed a great reduction in the hydrogen content, approximately 20 at.%. This result implies that hydrogen is extracted by MoS_2 powder under boundary lubrication conditions. MoS_2 is a catalyst that can form covalent bonds between sulfur and hydrogen so that hydrogen included in a-C:H surface can be extracted.

The specific wear rate increment of MoO_3 from room temperature to engine temperature shows it has a catalytic effect and changes the DLC structure chemically by breaking the chemical bonds of C-H, C-C, and also by element diffusion. This phenomenon is proved by the Arrhenius plot that consists of a specific wear rate as a function of inverse temperature. The slope of this graph determines the catalytic effect which leads to chemical wear. The slope values of Mo, MoO_3 and MoS_2 are much higher compared to MoDTC and Mo_2C, thus Mo, MoO_3 and MoS_2 promote chemical wear. The scratch marks found in the Mo_2C and mixed MoO_3+Mo_2C+Mo indicate that they promote abrasive wear.

After identifying all the behaviours of Mo-derived particles at room temperature and standard engine temperature, this research works concluded as follows. At first, MoDTC is degraded to MoS_2 and that MoO_3 is generated subsequently. The MoS_2 had the possibility of extracting hydrogen from the topmost surface. After several friction cycles from the beginning to the middle of the tests, the a-C:H surface may contain less hydrogen, and then MoO_3 can easily undergo tribo-chemical reactions with carbon atoms. Finally, Mo_2C generated and dispersed in the lubricant caused a much higher rate of wear by scratches than either MoS_2 or MoO_3 reacting with a-C:H.

ACKNOWLEDGEMENT

This dissertation is the culmination of studying Doctor of Engineering at Nagoya University, Japan. I have survived to finish my study with help and cooperation of many people. Alhamdulillah, a praise to The Almighty God for giving me chance and opportunity to accomplish this doctoral course.

First of all, I would like to immense gratefulness to my main supervisor, Associate Professor Takayuki Tokoroyama whose supervision, counsel and encouragement, from the preliminary to the concluding level enabled me to acquire a sound understanding of this research. He is an excellent Man of Example, not only in research, but also in my personal life. I am tremendously fortunate to be his doctoral student.

I would like to express my sincere gratitude to Professor Noritsugu Umehara for accepting me to be enrolled in his laboratory and Assistant Professor Motoyuki Murashima for their immense knowledge and guidance throughout my study.

I extend my deepest gratitude to the committee members, Professor Kenji Fukuzawa and Professor Hedong Zhang for sharing their brilliant ideas and thoughts, practical comments and suggestions to improve my thesis.

Of course a special thanks to the pillar of strength of my life, my lovely wife, Eleen Eleeda and my adorable daughter, Sakura Akira. Infinity thank you for your unlimited love and trust, support and care, and continuous prayers on me.

Infinity thank to my beloved father, Mohd Kassim Maarof, mother, Azizah Deraman and sister, Khairun Najwa for their endless love, prayers, moral support and encouragement lavished upon me. Their commitment and understanding has maintained my motivation to keep me giving 100% concentration.

I cannot end without convey my invaluable recognition to my doctoral course partner, Dr. Mohd Muhyiddin bin Mustafa for his knowledge, support, advice and guidance while finishing this project. It was a great moment working with him. Without all of these, this research project may not be completed.

Exceptional thanks also to Mr. Senda, for his technical support, and also to Ms. Sano and Ms. Kakizaki for their kindness giving me administrative support during the time in Umehara Laboratory.

Last but not least, thousands thanks to all my friends in Japan, especially Malaysian and Umehara Laboratory members for their help and support directly or indirectly throughout my life in Japan.

Finally, thanks to the Japanese Ministry of Education, Culture, Sports, Science, and Technology (MEXT: Monbukagakusho) for the full financial sponsorship for my doctoral study. Thank you Nagoya University for the facilities, hospitalities and experiences.

Contents

List of Figures

List of Tables

List of Formula

Chapter 1

Introduction

1.1 Tribology

Tribology is the science and technology of surfaces interacting in relative motion and includes the study and application of friction, wear, and lubrication. Figure 1.1 illustrates the basic principle of tribology. Among the most typical sliding and rolling components are gears, bearings, brakes, seals, and cams, which are widely used in machineries that have relative motion, including sliding motion or rotation [1-4]. Although this technology was initially designed to prolong the life of industrial machinery and extend their operation, it has evolved into a variety of other applications in which it has had a significant impact. In terms of research, tribology encompasses macro-scales to nano-scales [5].

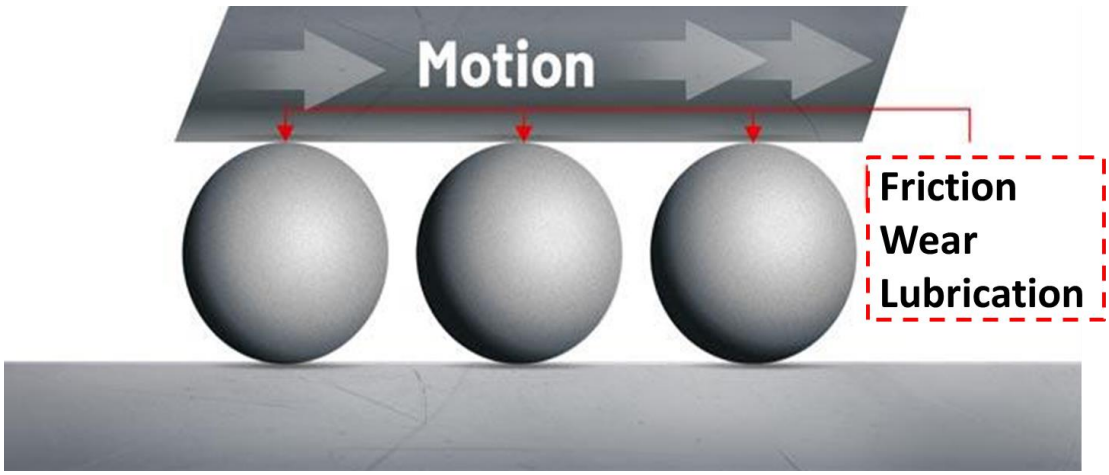

Figure 1.1 The principle of tribology

Traditionally, it has been focused on the transport and manufacturing sectors, but has become more diversified over time, and can now be divided into classical tribology, biotribology, green tribology, geotribology, nanotribology, tribotronics, space tribology, computational tribology, and open system tribology [6-13]. Since then, tribology has become an interdisciplinary field related to biology, chemistry, engineering, materials science, mathematics and physics. A comprehensive understanding of tribology begins with the definitions of friction, wear, and lubrication.

The definition of friction is the resistance to relative motion between two objects in contact. This occurs when charged particles on two surfaces that are touching are attracted by the electromagnetic field. Meanwhile, wear occurs when material is removed, damaged, or displaced from solid surfaces. Lubrication is the process of creating a film between moving surfaces in contact that reduces friction and wear. Generally, lubricants can be solid, fluid or plastic, with oil or grease being the most common fluids [13-14].

1.2 Wear

Wear refers to the removal of material or surface damage caused by the sliding, rolling or impact motion of surfaces relative to each other. The wear typically occurs at asperities of interacting surfaces. As a result of relative motion, the material at the interacting surfaces can be removed. This may lead to some changes of material properties at least at the interface region, though there is a likelihood of very little or no loss of material [15]. Then, the removed material at the interacting surfaces may relocates and transfers to the counterpart surface or may break into tiny wear debris.

The wear occurs chemically or mechanically which is normally accelerated by frictional heating. The wear consists of six basic classification with a quite distinct phenomena and complex interaction between each other. The most common wear can be classified as follows: (1) abrasive; (2) adhesive; (3) fatigue; (4) fretting; (5) erosive; (6) oxidation wear [16-18]. However, the wear such as abrasive, adhesive and oxidation are the major combinations of wear. Based on the previously encountered issues, the abrasive and adhesives are the major wear mechanisms in the industry.

Abrasive wear described as material loss caused by hard particles being forced against and moving along a solid surface. It happens when a hard rough surface or hard particle slides or rolls over a softer surface as shown in Fig. 1.2. The hard particle may be 'foreign' particles caused by adhesive or delamination wear. Micro-scale cutting and plowing processes commonly take place in abrasive wear [19]. The intensity of abrasive wear is resolved by the way of asperities slide or roll over their mating surface.

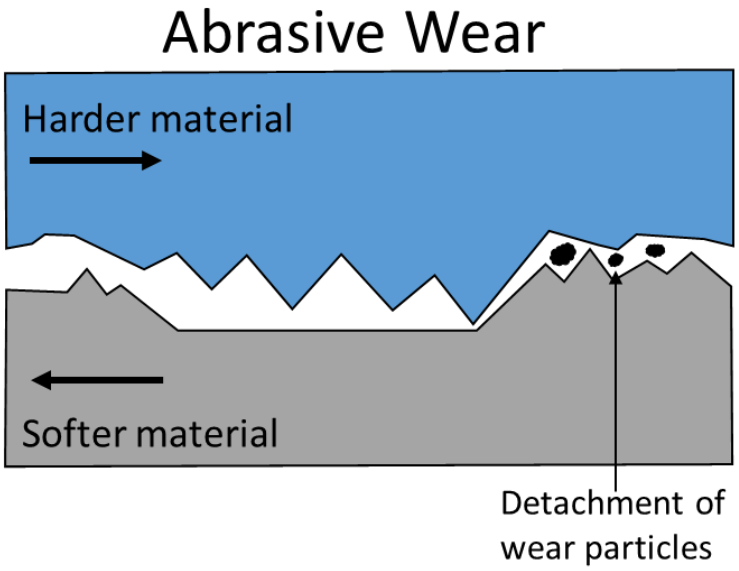

Figure 1.2 The fundamental of abrasive wear

Adhesive wear refers to the bonding of asperities or surface roughness between two sliding material surfaces. Instantaneous micro-welding occurs at the material surfaces caused by the heat generation from the friction as depicted in Fig. 1.3. As a result, detachment or material transfer take place between surfaces [20-21]. In order for adhesive wear to occur, the surfaces must be in close contact to one another. This may result in undesirable wear debris and material compounds being displaced and attached from one surface to another. Adhesive wear also can cause increment of surface roughness and protrusions on the material surfaces.

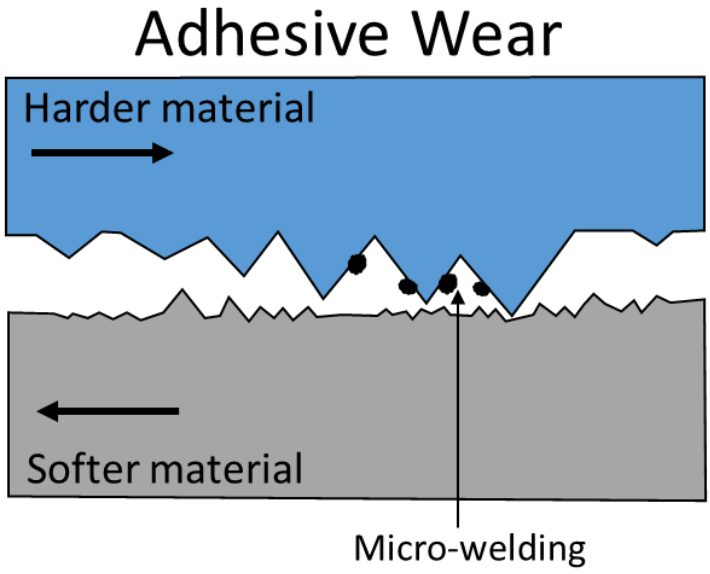

Figure 1.3 The fundamental of adhesive wear

1.3 Diamond-like Carbon

Diamond-like carbon (DLC) is a kind of amorphous carbon material that gives some of the diamond's typical properties. In 1971, the signature of DLC was first introduced by Aisenberg, to characterize the hard carbon films produced by direct deposition from low energy carbon ion beams [22]. In 1980s, the DLC was started to receive vast attention for comprehensive research [23].

Since it has similarities to the natural diamond in term of its mechanical, chemical, electrical and optical properties, it offers tribological benefits to many industries. Usually scale in between 1 μm to 4 μm of thickness, DLC also has broad-ranging properties. The primary aspect that regulate its properties is the proportion of graphite-bond (sp^2) to the diamond-bond (sp^3) carbon atoms. It is also dependent to other factors like the presence of nitrogen, hydrogen, silicon and metal dopants.

There are three different bonding configurations of Carbon with single bond, double bond and triple bond, particularly sp^3, sp^2 and sp^1 as depicted in Fig. 1.4 [24]. The hybridization of graphite sp^2 and diamond sp^3 formed a DLC as shown in Fig. 1.5 [25]. Diamond has four sp^3 hybridized orbitals which contribute to the formation of four equal carbon-carbon bonds with adjacent atoms, which produces the tetrahedral structure of diamond.

This covalently bonded tetrahedral structure is the origin of the superior properties of diamond, like high hardness and high thermal conductivity. Meanwhile, graphite has three trigonally directed sp^2 hybrid orbitals, which lie in plane. Each carbon atom in plane is bonded to three other carbon atoms with strong covalent bonds. The layers of carbon atoms are attracted to each other by weak Van der Walls forces

producing the layered structure of graphite. The layers can cleave easily, which accounts for the typical low friction property of graphite [26-27].

The DLC films have a mixed sp^3/sp^2 structure with different proportions of sp^3 and sp^2 bonds depending on the deposition techniques and deposition parameters used. The structure is claimed to consist of sp^2 bonded clusters embedded in an amorphous sp3 bonded carbon matrix [28-29]. So the term "diamond-like" emphasizes a set of properties akin to diamond and, at the same time implies the absence of crystalline diamond order [30].

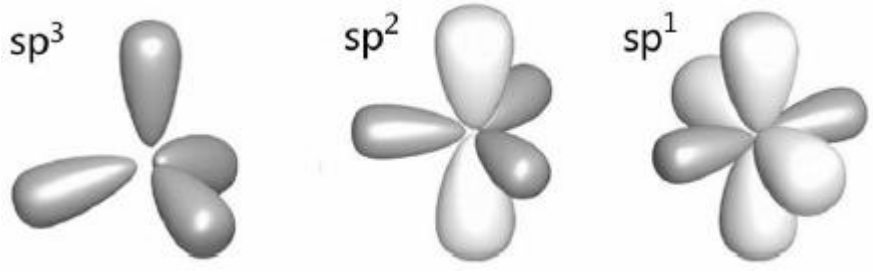

Figure 1.4 Three different bonding configurations of Carbon [24]

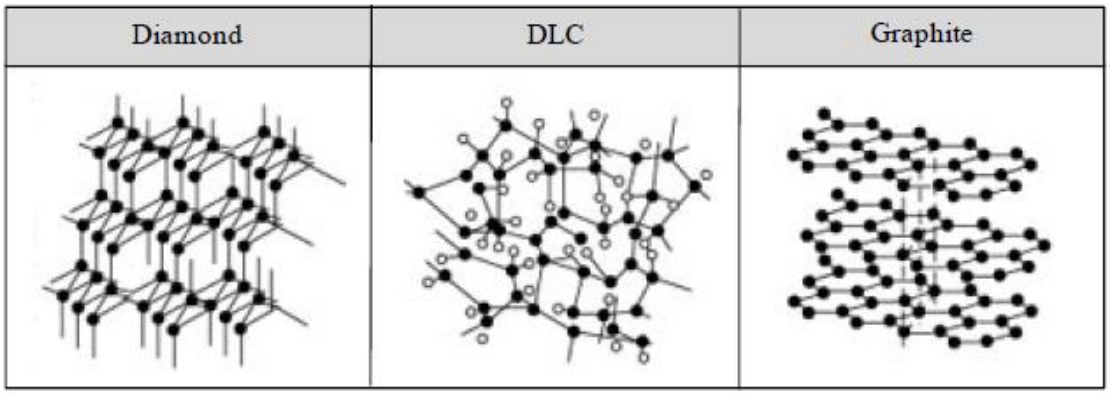

Figure 1.5 The structure DLC from hybridization of diamond sp^3 and graphite sp^2 [25]

There are variety of DLC has been introduced such as hydrogen-free tetrahedral amorphous carbon (ta-C), hydrogen-free amorphous carbon (a-C), hydrogenated

amorphous carbon (a-C:H), hydrogenated tetrahedral amorphous carbon (ta-C:H) and doped DLC like Si-DLC and Me-DLC [31-34]. Those DLC have their own characteristics and valuable properties such as great wear resistance due to high hardness, low friction coefficient, chemical stability, electrical insulation, optical transparency and also biological compatibility.

Therefore, DLC become one of the potential candidates for coating material due to its excellent properties and feasible for many application as illustrated in Fig. 1.6 [35-36]. Tribology of DLC discusses important structural, chemical, mechanical and tribological characteristics of DLC films. Particularly dedicated to the fundamental tribological issues that impact performance and durability, this description covers a variety of industrial applications, including automotive, microelectronics, aerospace, biomedical, textile, and manufacturing.

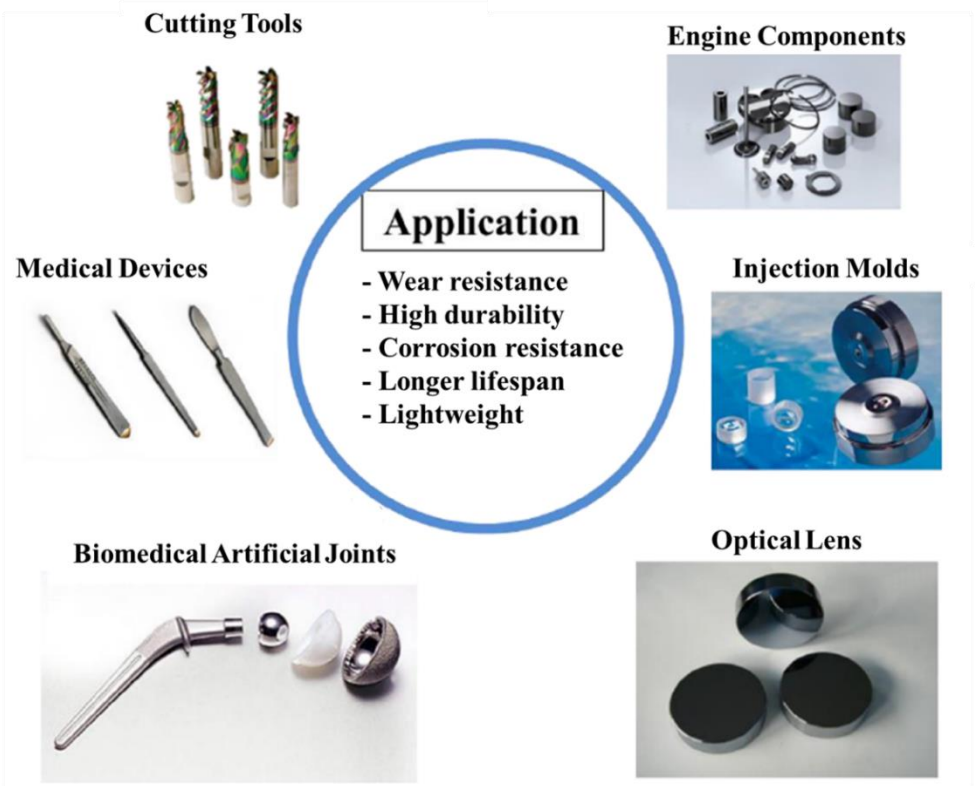

Figure 1.6 Various applications of DLC coatings

1.4 Lubrication

In actual condition of automotive engine, the speed and the load of the engine components are constantly changing and varies, thus working in all lubrication regimes. Lubrication regimes consist of hydrodynamic lubrication, mixed lubrication and boundary lubrication. The friction and wear of an engine is highly dependent on the lubrication regimes as shown on the Stribeck Curve in Fig. 1.7 [37].

The friction coefficient and the lubricating film thickness are plotted as a function of velocity, fluid viscosity and load. The lubricating film thickness between solid-to-solid surfaces determines the lubrication condition. Among these three regimes, boundary lubrication is the severest lubrication condition and lead to a higher friction and wear. It always existed during start and stop, shock-loads or changing in direction.

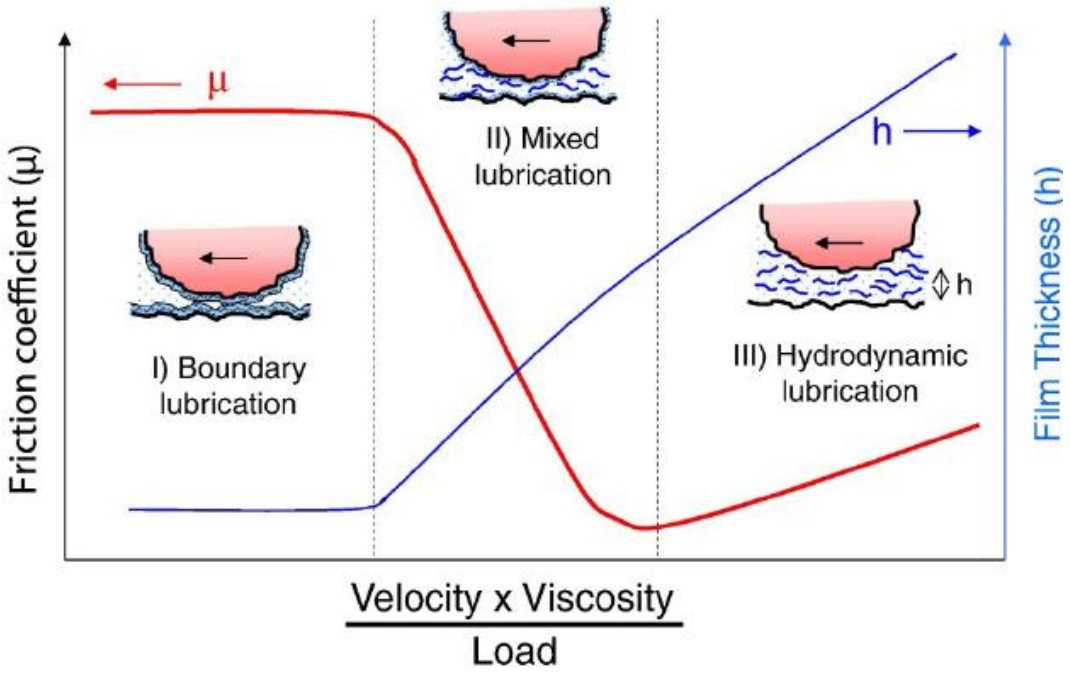

Figure 1.7 Stribeck curve and lubrication regimes [37]

Since DLC coating performed excellently to give low friction and long life span due to its high hardness and chemical inertness properties, it is now being prominently used in automotive industry as coating materials especially on the sliding parts of automobile engine such as piston ring and cylinder liner [38-41]. However, they are operating under severe boundary lubrication condition which lead to higher friction and wear losses. The high friction and wear contribute to the loss of energy generated by automobile engine. Therefore, high surface technology such as DLC is implemented and working together with lubricant additives to improve efficiency, durability and sustainability of the engine.

Commonly, lubricants are blended with roughly around 10% of additives combo to enhance their lubricating capabilities under boundary and mixed lubrication regimes. Each additives have their own special functions to the lubricant such as friction modifier, anti-wear, antioxidants, viscosity improvers, detergents, corrosion inhibitors, emulsifier, and extreme pressure additives as illustrated in Fig. 1.8 [42].

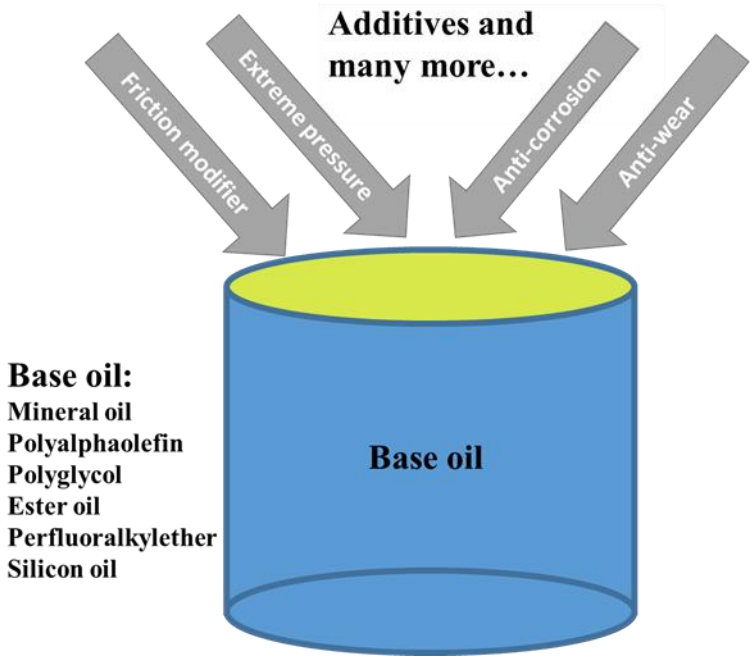

Figure 1.8 Lubricant with additives combo

1.5 Additive Effects on The Wear of DLC

Numerous DLC-coated automobile engine parts have to run against steel counterpart in actual working condition. The lubrication of such DLC/steel contact is a complicated system with variety of parameters affecting the operation. For further development and sustainability of the engine, the effects of lubricant additives to DLC coatings on the contact parts are extensively being studied in order to get the optimum operating condition especially under the boundary lubrication regime [43-52].

A decade ago, the initial studies of friction and wear for additive-free lubrication of DLC coatings were reported by Nevile et al. and Kalin et al. The contradictory of boundary lubrication in term of tribological performance and tribofilm formation were carefully reviewed [48, 53]. Masripan et al. explored the effect of hardness on the DLC coating lubricated in additive-free mineral base oil and concluded the hardest DLC gave the lowest friction and wear [54]. Meanwhile, Vengudusamy et al. investigated different types of DLC coatings under API III base oil lubrication. They found that the ta-C coatings gave lower boundary friction than any other DLC coatings and the wear resistance is dependent on the DLC type [55].

These days, the studies on the lubricant additives effect to DLC coatings have captured tremendous attention. De Barros'Bouchet et al. and Yue et al. investigated that hydrogenated DLC (a-C:H) coatings undergo super-low friction in the lubricant that contained friction modifier, Molybdenum Dithiocarbamates (MoDTC), affected by the formation of self-lubricating MoS_2 films [46, 56]. MoDTC is very proficient in reducing the friction coefficient between DLC/steel contact surfaces under boundary lubrication [57-58]. However, Vengudusamy found that MoDTC degrades wear

resistance greatly for DLC-steel contact and many other researchers too determined that the wear rate DLC coatings were higher in MoDTC-contained lubricant compared to pure base oil lubrication [59-76]

The wear performance of DLC coatings under boundary lubrication can be improved by dispersing Zinc Dialkyldithiophosphate (ZDDP/ZnDTP) additive [64, 77] into lubricant. ZDDP is a well-known anti-wear additive in lubricating oil formed a protective tribofilm on ferrous surfaces during tribo-chemical reactions [78]. Heau et al. also concluded that with addition of 1% glycerol mono-oleate (GMO) additive into base oil gives a substantial improvement in wear behaviour especially for the hydrogen-free DLC [79].

Therefore, in order to have better understanding about the wear effect of friction modifier additive towards DLC-steel counterpart under boundary lubrication condition, the behavior of MoDTC must be particularly studied.

1.6 Degradation of MoDTC and Mo-derived Materials

MoDTC has received noticeable attention as an anti-friction additive in automobile lubrication. MoDTC is very proficient in reducing friction coefficient between DLC-steel contact surfaces under boundary lubrication. However, lubrication with MoDTC lead to a high wear of DLC. MoDTC is a degradable material and easily change its physical and chemical structures [80-85].

It is often assumed that the intermediate and final products from the degradation of MoDTC as the wear acceleration material. These compounds increase the wear of DLC coating. There are several by-products compounds from the MoDTC degradation

has been discovered; molybdenum trioxide (MoO_3), molybdenum carbide (Mo_2C), molybdenum disulfide (MoS_2) and pure molybdenum (Mo). However, which compound mainly accelerates the wear is still questioned.

Previous research works presumed that the intermediate products from the degradation of the liquid MoDTC accelerate the DLC wear. Mo-derived compounds such as MoS_2 and MoO_3 were reported to form tribo-layers on hydrogenated DLC and promote chemical wear [67-68]. The other Mo-derived compound, Mo_2C is revealed to cause an abrasive wear on DLC surface [67]. On the other hand, Mo tribofilm formed from the MoDTC degradation also contribute to the wear acceleration by chemical-adhesive wear [66].

1.7 Wear Acceleration Mechanism

Based on the previous findings by researchers, the wear acceleration mechanism from the MoDTC degradation were classified into several categories.

Okubo et al. considered the wear acceleration of DLC coatings under MoDTC lubrication was caused by two factors: the chemical wear caused by the tribo-chemical reactions between Mo compounds derived from MoDTC and DLC surfaces to produce Mo_2C and the abrasive wear caused by Mo_2C particles. Figure 1.9 shows the proposed wear acceleration mechanism of a-C:H lubricated with MoDTC solution. However, no additional analysis proved the detailed mechanism of the wear acceleration of DLC coatings under MoDTC lubrication [67].

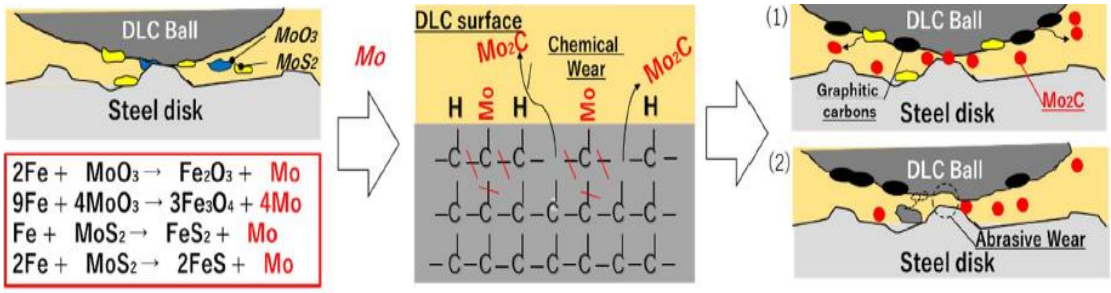

Figure 1.9 The proposed wear acceleration mechanism by Okubo [67]

Meanwhile, Ohara et al. proposed that a chemical wear took place to accelerate wear of DLC coatings against steel counterpart under MoDTC lubrication due to the oxidation of MoO_3 from the MoDTC degradation which then make a structural transformation to sp^2 from sp^3 on DLC surface [68]. Figure 1.10 illustrated the proposed wear mechanism.

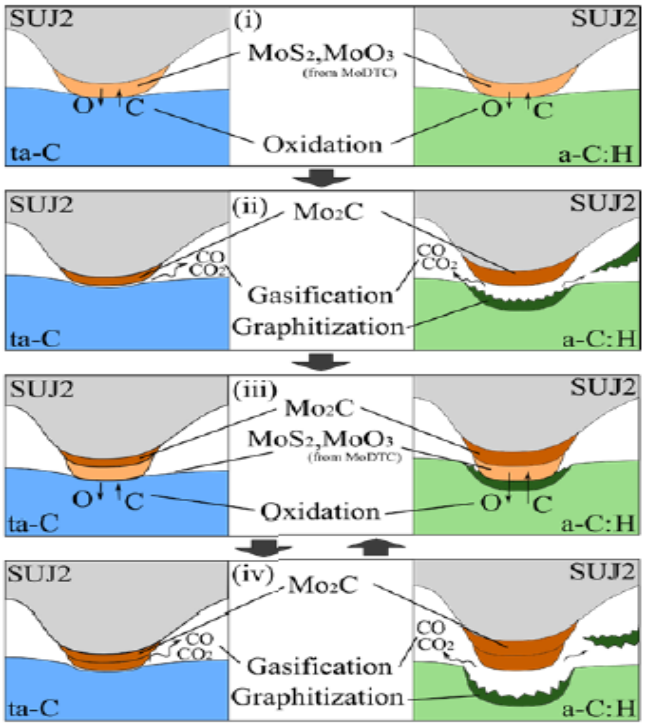

Figure 1.10 The proposed wear acceleration mechanism by Ohara [68]

On the other hand, De Feo et al. stated that adhesive wear due to chemical reaction happened under MoDTC lubrication accelerates the wear of DLC. MoDTC was decomposed into to form Mo tribofilm on the steel counterpart and then adhere carbon from the dangling-bond of DLC to form Mo_2C [66]. The wear acceleration mechanism was proposed in Fig. 1.11.

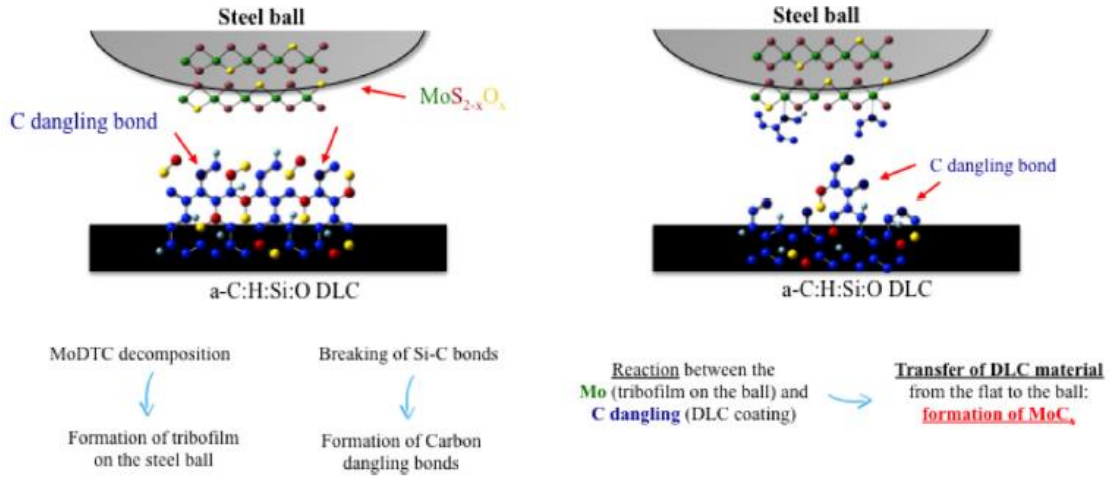

Figure 1.11 The wear mechanism model prospected by De Feo [66]

1.8 Surface-enhanced Raman Scattering (SERS)

The surface analysis of lubricant additives effects on DLC coatings and the proposed wear acceleration mechanism must be conducted carefully and accurately. Generally, Raman analysis is widely practiced to collect structural data of carbonaceous coatings. The defect density of the structure is usually identified by the intensity ratio (I_D/I_G) and the positions of disordered D-peak and graphite G-peak [86]. However, this normal Raman analysis gains data in several μm depth, including the coating's substrate. Harima has reported that through laser excitation wavelength of 532 nm by Raman spectroscopy, the detection depth is within 300-600 nm [87].

One of the enhancement procedure to collect more accurate and systematic structural surface information is by using surface-enhanced Raman scattering (SERS) analysis. The SERS analysis helps to improve the depth resolution, by gathering only the topmost surface structural data [88-89]. The SERS procedure is conducted by scattering gold nanoparticles (AuNPs) onto the coating surface. The AuNPs reacts as localized surface plasmon resonance (LSPR) which optimizes the reflective wavelengths [90-94].

Figure 1.12 shows the comparison between (a) normal Raman analysis and (b) SERS analysis. For normal Raman procedure, the incident wavelength penetrates the coating until reach the substrate. The dotted-circle illustrates the area of structural data gathered. For SERS, the AuNPs prevent the incident wavelength to enter deeper into the coating and substrate. Thus, the structural information is only obtained at the topmost surface in several nanometer depth.

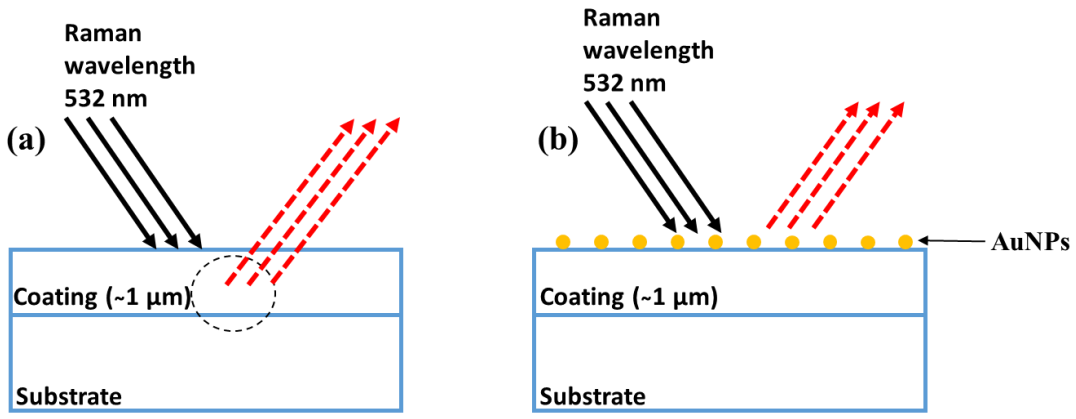

Figure 1.12 Comparison between (a) normal Raman and (b) SERS procedures

1.9 Scope of Study

According to previous studies elaborated in above sections, there are a lot of conclusions and assumptions being made about the MoDTC degradation. However, which Mo-compound precisely accelerates the wear; either MoDTC itself or the Mo-derived compounds from the MoDTC degradation has still been unclear. This complex condition is quite critical especially in automobile engine parts as the wear will shorten the lifetime of DLC. Further analyses are required to identify each Mo-derived compound effect and their playing role to enhance wear. At this stage, it is not necessary to identify the wear acceleration mechanism, but the most important thing is to study the behavior of each Mo-derived compound and then classify their wear effect on DLC.

Therefore, powder-type MoDTC and Mo-derived (MoO_3, Mo_2C, MoS_2, and Mo) compounds should be used to understand the particular effects each of them. They should be dispersed into base oil and tribologically tested on DLC-steel contact under boundary lubrication in the room temperature of 23 ºC and standard operating engine temperature of 80 ºC. In Chapter 2, the focus point is to classify the friction and wear effect of Mo-derived particles on two different DLC coatings. From here, the compound that plays major role in accelerating wear of DLC can be identified.

Then, the studies continued in Chapter 3 to understand the tribological behaviours of Mo-derived compounds and their mixing effect at standard operating engine temperature. Further Raman analysis by implementing SERS procedure is conducted to accurately figure out the wear acceleration effect each of the Mo-derived particles. Figure 1.13 illustrates the outline of this dissertation.

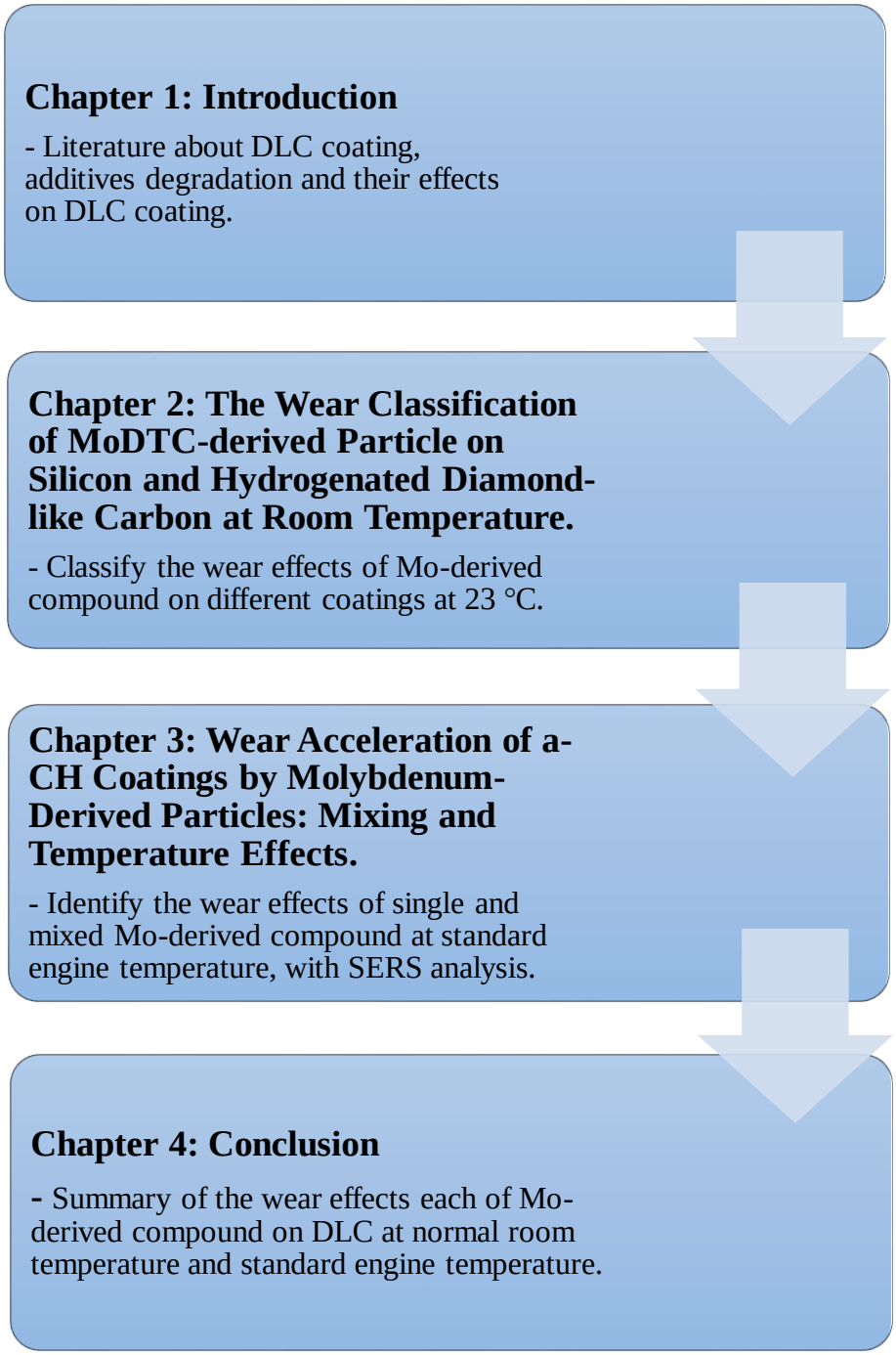

Figure 1.13 The outline of dissertation

Chapter 2

The Wear Classification of MoDTC-derived Particles on Silicon and Hydrogenated Diamond-like Carbon at Room Temperature

2.1 Introduction

Since decades ago, the control of friction and wear in the automotive engine system has been captured attention by many researchers. Low friction coefficient under boundary lubrication that leads to a vital decrement of fuel consumption, and also an increment of life expectancy and durability of engine parts are the main goals of those researches [23, 62, 95].

Diamond-Like Carbon (DLC) coating is one of the potential candidates to give low friction and long life span due to its high hardness and chemical inertness properties [96-97]. It is now being prominently used in industry as coating materials. The low friction property of DLC under boundary lubrication is a paramount factor on the sliding parts of automobile engine especially on piston ring and cylinder liner [38-41].

In the automotive industry, the effect of lubricant additives to DLC coatings on the contact parts have been extensively studied in order to get the optimum operating

Condition under lubrication regimes [43-45]. In recent years, molybdenum dithiocarbamate (MoDTC) has received noticeable attention as a friction modifier additive in automobile lubrication.

MoDTC is very proficient in reducing the friction coefficient between DLC/steel contact surfaces under boundary lubrication [57-58]. However, the MoDTC lubrication resulted in wear increment of DLC [46, 64]. MoDTC is an easily degradable material and can simply change its physical and chemical structures [65].

It is often assumed the intermediate and final products from the degradation of MoDTC as the wear acceleration material. These compounds increase the wear and scratch both DLC and the counterpart surfaces. Previous research works already summarized that MoDTC increases the DLC wear because of several reasons. It was proposed that chemical wear and abrasive wear took place from the interaction of MoDTC-derived compounds [66-67].

Some of them also suggested that molybdenum trioxide (MoO_3) degraded from MoDTC leads to chemical wear [59, 68]. It can be summarized that there are several by-product compounds from the MoDTC degradation has been discovered previously; MoO_3, molybdenum disulfide (MoS_2), molybdenum carbide (Mo_2C), and pure molybdenum (Mo).

However, which compound and when it mainly accelerates wear of DLC has not been fully understood. Thus, it is very essential to identify which Mo-derived compound affects the wear of DLC. This complex condition is quite critical especially in automotive components as the wear will shorten the lifetime of DLC. Therefore, further analyses are required.

This chapter focused on the classification of the wear acceleration effect on the hydrogenated amorphous carbon (a-C:H) DLC by the Mo-derived particles, especially for MoDTC, MoO_3, Mo_2C, MoS_2 and pure Mo (so-called the 5 different particles) because they were reported as a by-product of MoDTC degradation. Friction tests were conducted only 1500 cycles under room temperature to eliminate a possibility of Mo-derived materials' degrade during the tests.

Then, the wear amount of a-C:H were compared to Silicon-doped type a-C:H (so-called Si-DLC). This is to reveal that Si-contained DLC gives significant effect for tribological properties. The features of wear track on DLC surface and its width were observed by Field Emission Scanning Electron Microscope (FESEM), and then the structural change of DLC was obtained by a Raman spectroscopy.

2.2 Experimental Procedure

The friction tests were conducted by using a Ball-on-disc type friction tester. It has stainless steel leaf springs with strain gauges as a load sensor and a friction force sensor to measure the normal load and friction force. The load sensor was connected to the X-Z stage, and the normal load was applied by pressing a counter material by Z-axis position change.

The strain of normal load and friction force was magnified by the strain amplifier to a voltage value, the value was transmitted to PC through data logger as 10 data per second (sampling frequency was 10 Hz). Figure 2.1 (a) illustrates the whole friction test setup and Fig. 2.1 (b) shows the Ball-on-disc position during the sliding test.

The counter material being used was SUJ2 (high-carbon chromium bearing steel) ball with diameter 8.0 mm against two different DLC-coated discs, which were hydrogenated amorphous carbon (a-C:H DLC) and silicon-doped a-C:H (Si-DLC). Both DLC were prepared by using chemical vapor deposition (CVD) method in the same chamber on the substrate of silicon wafer (Si (100)).

The coating hardness for a-C:H was approximately 18.0 GPa, and for Si-DLC was approximately 25.0 GPa, tested by Nano-indentation hardness tester (Nano-indentation tester, Elionix ENT-1100a). The roughness for a-C:H was R_a=1.0 nm, and for Si-DLC was R_a=0.9 nm, quantified by atomic force microscopy (AFM, SPM-9700HT). Both DLC have the same coating thickness which was approximately 0.5 µm. Poly-alpha-olefin (PAO) with viscosity 19.0 mm^2/s was used as the base oil in this study.

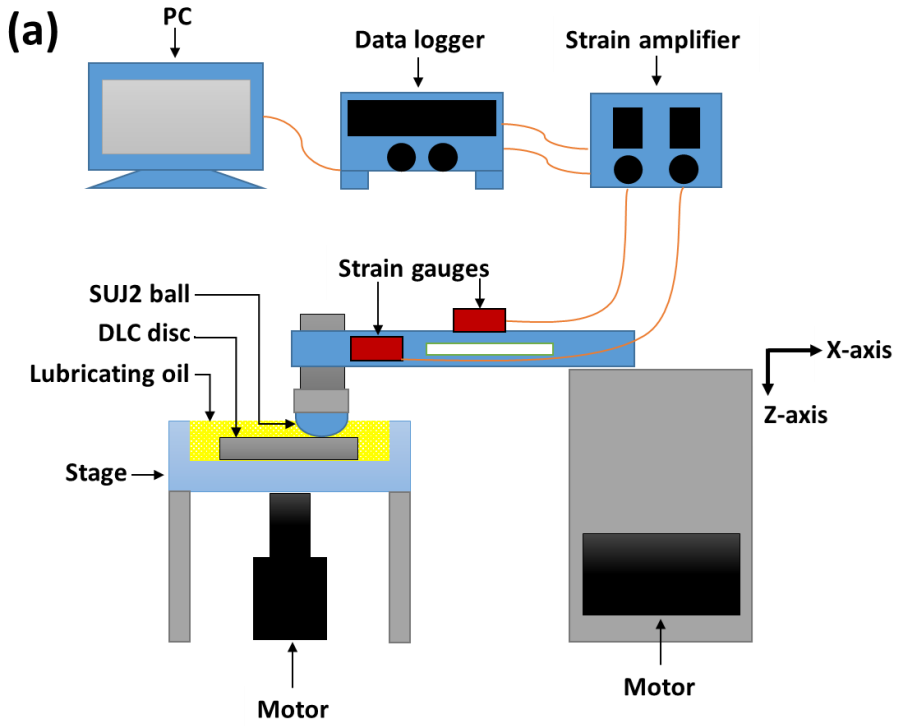

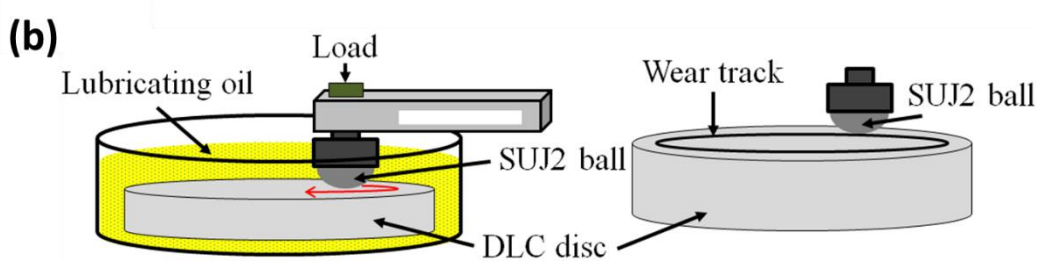

Figure 2.1 The schematic images of (a) the Ball-on-disc friction tester and (b) the ball-on-disc position during the sliding test

All the 5 different particles; MoDTC, MoO_3, Mo_2C, MoS_2, and Mo which have size between 2.0 to 5.0 μm were dispersed into the PAO base oil with 0.1% volume percentage, respectively. The FESEM images of these particles are shown in Fig. 2.2 (a) to (e), respectively.

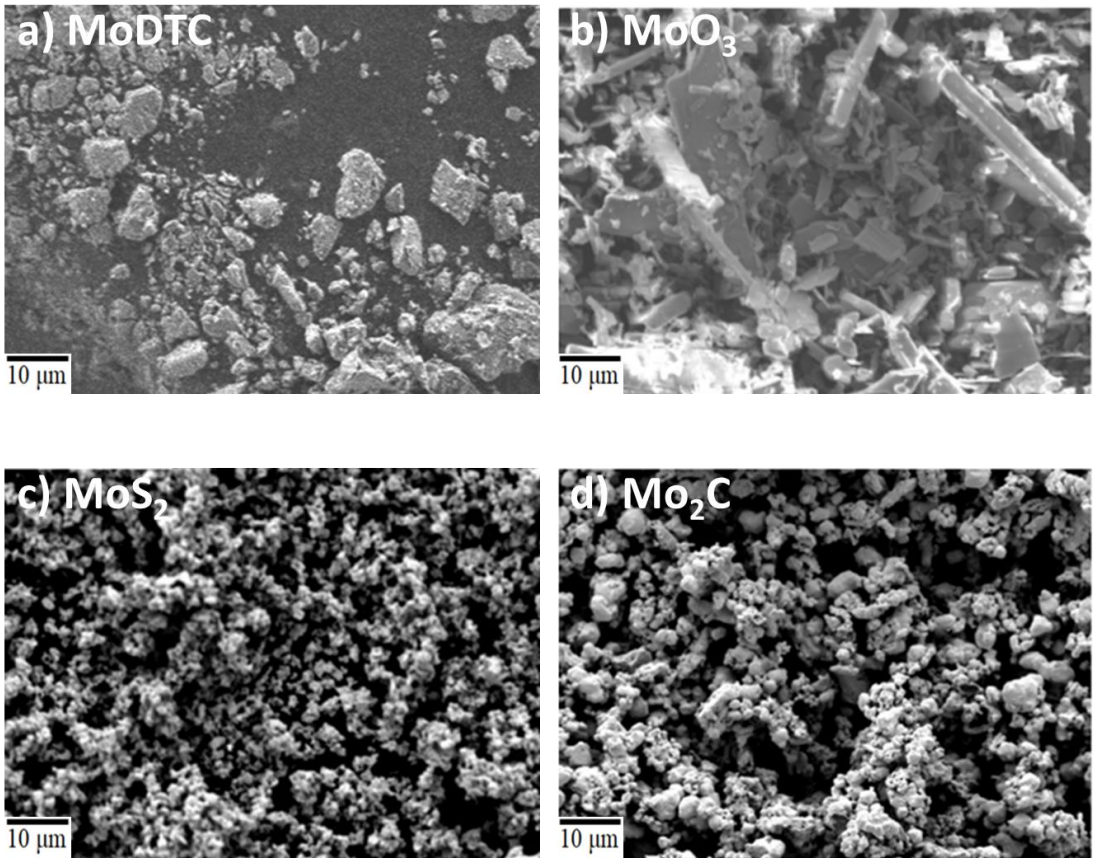

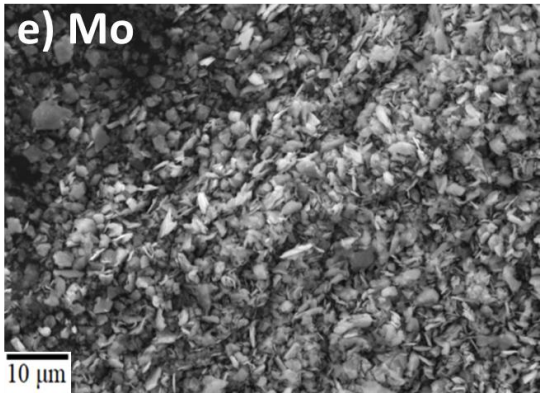

Figure 2.2 FESEM images of powder-type particles (a) MoDTC, (b) MoO_3, (c) MoS_2, (d) Mo_2C and (e) pure Mo.

MoDTC, Mo_2C, MoS_2, and Mo were provided from the conventional material supplier in the industrial field. Only MoO_3 was experimentally synthesized from MoS_2 in the laboratory. To ensure the real MoO_3 was synthesized, Raman analysis for both MoO_3 and MoS_2 were conducted.

The result in Fig. 2.3 shows the two sharp peaks on the MoS_2 line indicated that it was a pure MoS_2. Meanwhile, several peaks on the MoO_3 line proved that it was pure, as it was merged the MoO_3 peaks conducted by Windom et al. in the previous finding [69]. The hardness of each particle were as follows; MoDTC (1.0 GPa), MoO_3 (2.5 GPa), Mo_2C (15 GPa), MoS_2 (1.0 GPa), and Mo (1.5 GPa).

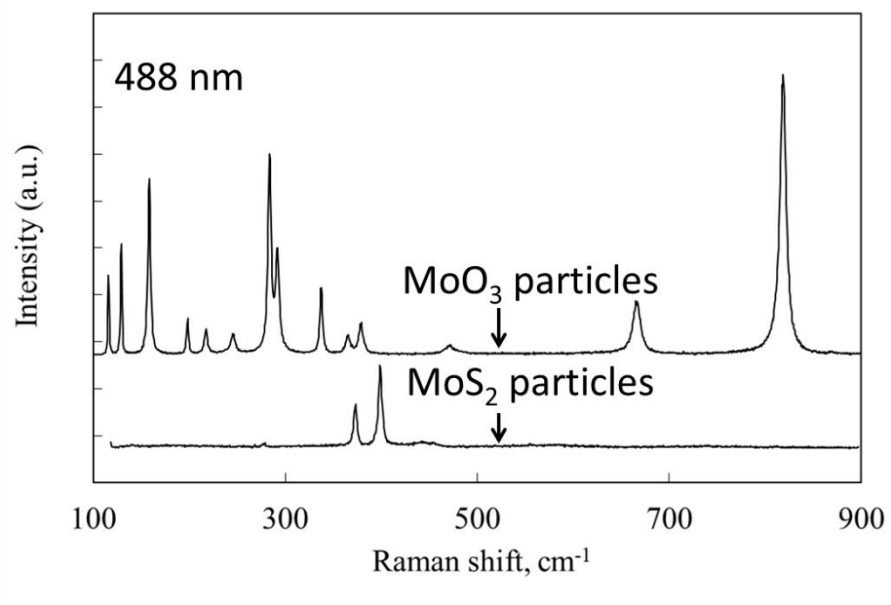

Figure 2.3 The Raman analysis data of MoO_3 and MoS_2

The mixtures of PAO base oil with the 5 different particles were stirred in the ultrasonic bath for at least one hour before starting the friction tests to ensure no particles settlement and an uneven mixture. The tests were run for 1500 cycles in 15 minutes with 0.05 m/s speed at 23°C under an applied load of 1.0 N corresponds to the maximum initial Hertzian contact pressure of 455 MPa.

All samples were cleaned with benzene, then acetone in an ultrasonic bath before and after friction test to remove the oil stains and contaminants. Then, the wear of DLC discs was observed by using an optical microscope and FESEM (JEOL, JSM-7000FK), and then continued by Raman spectroscopy (Renishow) under 488 nm wavelengths and 0.5 mW output beam within the range of 800-2000 cm^{-1}.

2.3 Results

2.3.1 Friction coefficient of a-C:H and Si-DLC disc with 5 different particles under boundary lubrication

The friction coefficient results of a-C:H disc and Si-DLC disc against SUJ2 ball with a dispersion of the 5 different Mo-derived particles (MoDTC, MoO_3, Mo_2C, MoS_2, and Mo) into PAO base oil are shown in Fig. 2.4 (a) and (b), respectively. All friction tests were run with a dispersion of 0.1 vol.% particles. The steady-state friction coefficients at the final 500 cycles before the friction test ends were taken as the average friction coefficient and the results were summarized in Fig. 2.5.

At first, the friction test of a-C:H and Si-DLC discs were run under lubrication of PAO base oil only, without any dispersion of the 5 different particles. Both discs show the lowest friction coefficient, around 0.05. Based on the variation of friction coefficient, it shows that the running-in period took place from the initial period until 200 cycles before they achieved a stable friction trend. The 5 different particles showed divergent friction coefficient on the two different DLC discs.

For a-C:H, MoO_3 showed the most effective particle to increase the friction coefficient to approximately 0.17. MoDTC and MoS_2 showed almost the same lowest value at approximately 0.10. On the other hand, Mo_2C and Mo indicated a friction coefficient of nearly 0.12 and 0.14, respectively.

For Si-DLC, Mo contributed to the highest friction coefficient about 0.13, and MoDTC had an effect to the utmost friction reduction approximately at 0.09. Mo_2C showed a moderate friction coefficient at around 0.12 after the running-in period until the end of sliding cycles. The stable friction coefficient of Mo_2C for both DLC discs was quite contrasting with the other particles which had fluctuation throughout the sliding period.

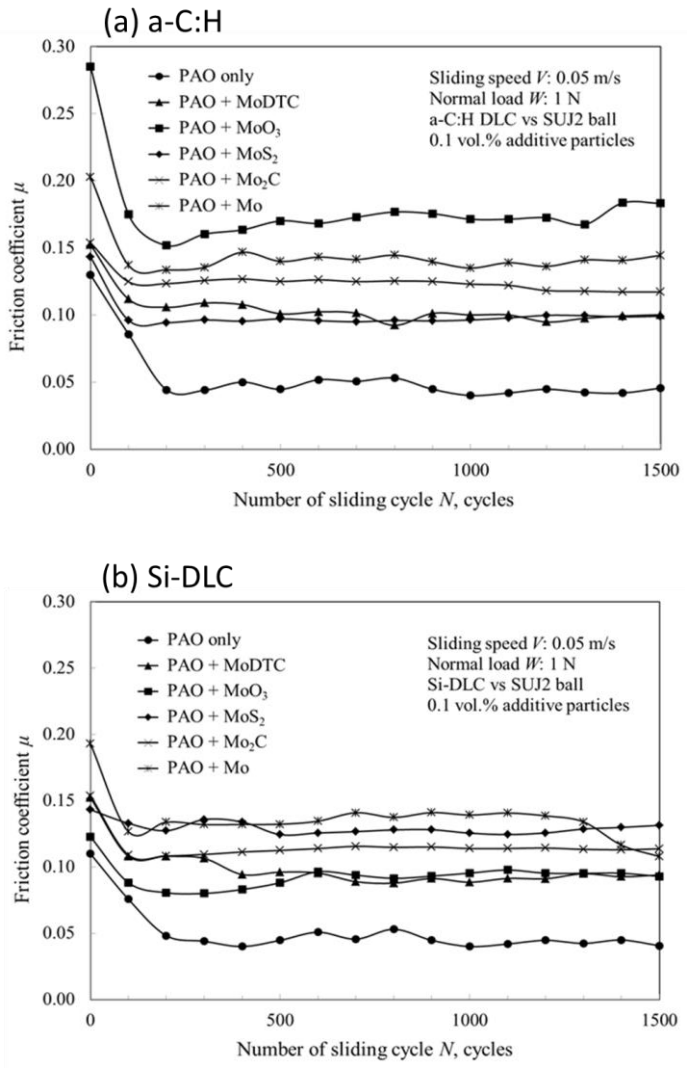

Figure 2.4 Variation of friction coefficient as a function of sliding cycles, (a) a-C:H and (b) Si-DLC against SUJ2 ball under 5 different particles contained lubrication condition

The comparison in Fig. 2.5 shows the 5 different particles basically had a lower friction coefficient on Si-DLC disc. For example, MoO_3 reduced almost half of its friction coefficient on Si-DLC. MoDTC, Mo_2C, and Mo also indicated a slight friction reduction from a-C:H to Si-DLC. At the same time, MoDTC played its main role as a friction modifier since it had the lowest friction coefficient for both discs. However, MoS_2 presented a higher friction coefficient on Si-DLC compared to a-C:H disc.

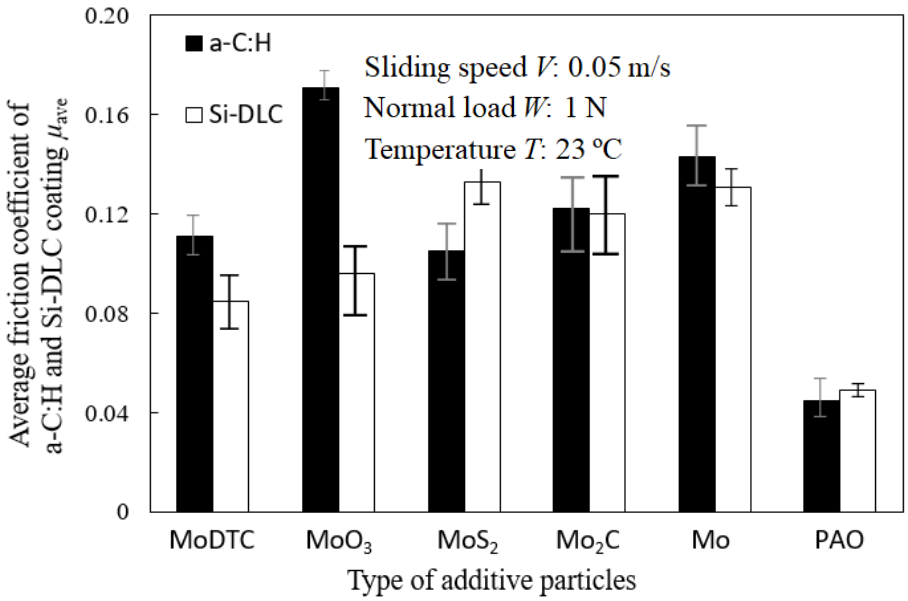

Figure 2.5 Average friction coefficient of a-C:H and Si-DLC coating against SUJ2 ball under 5 different particles contained lubrication condition

2.3.2 FESEM observation of wear track on DLC discs

FESEM observations were conducted onto the surfaces of a-C:H and Si-DLC discs. Figure 2.6 shows the effect of the 5 different particles on wear track of the a-C:H discs after the friction test against the SUJ2 ball, respectively. Mainly, only MoDTC and Mo_2C showed severe wear effect onto the a-C:H disc. Referring to Fig. 2.6 (a) of MoDTC, the DLC/steel contact area delaminated, but was confirmed not reaching the substrate. The enlargement image on Fig. 2.6 (a') showed crescent-shape wear. Figure 2.6 (b), (c) and (e) revealed MoO_3, MoS_2, and Mo only showed a small and shallow wear track, respectively. Their surfaces also looked the same inside and outside of the wear track. This meant that the original a-C:H coating was not worn-out during the friction test. On the other hand, severe scratches took place on the a-C:H disc for Mo_2C as shown in Fig. 2.6 (d). Based on its enlargement images Fig. 2.6 (d'), there were layers of coating flakes peeled-off from the surface.

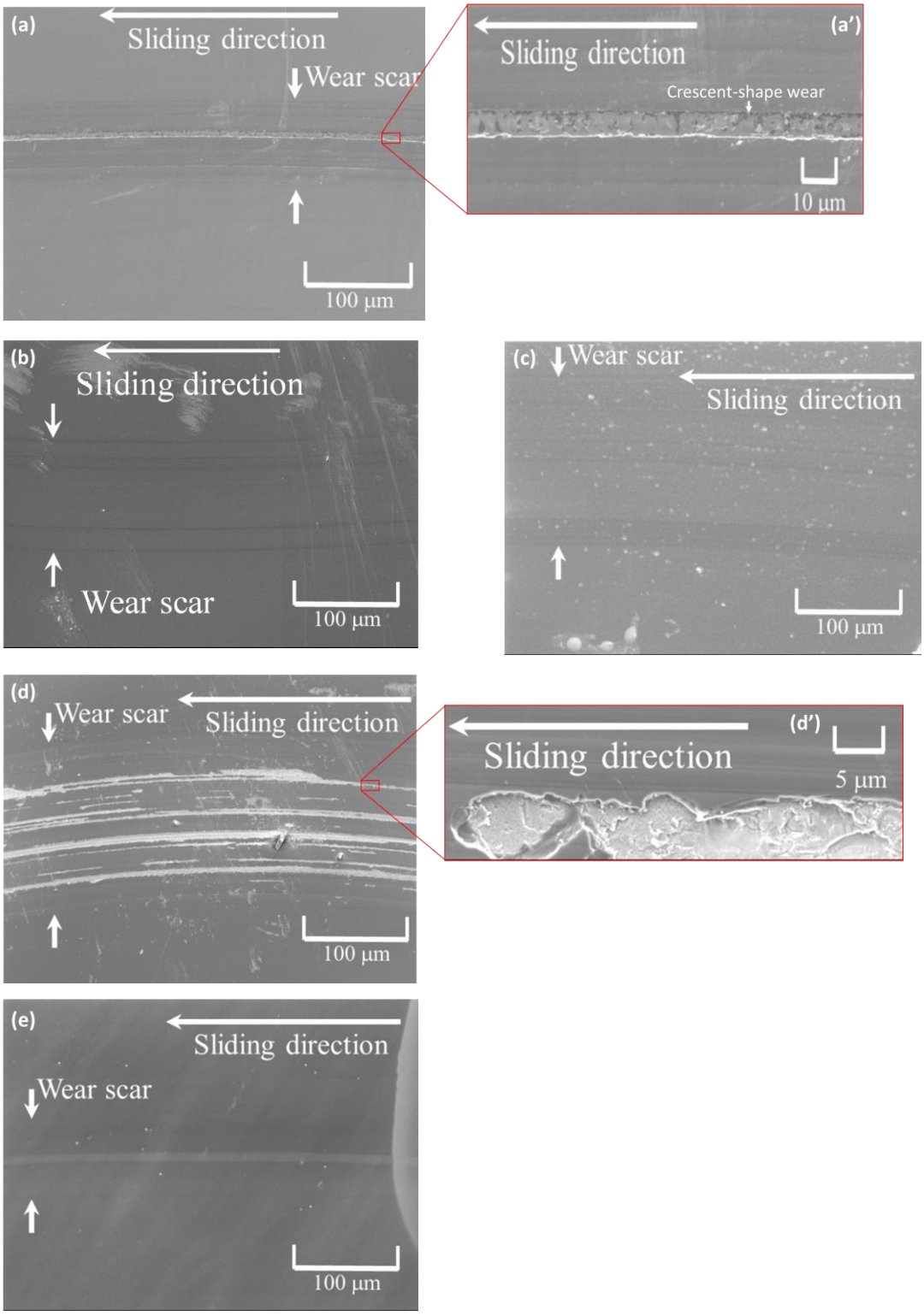

Figure 2.6 FESEM images of wear track on a-C:H disc against SUJ2 ball under lubrication of (a) MoDTC and (a') enlargement of the surface, (b) MoO_3, (c) MoS_2, (d) Mo_2C and (d') enlargement of the surface, and (e) Mo with PAO oil

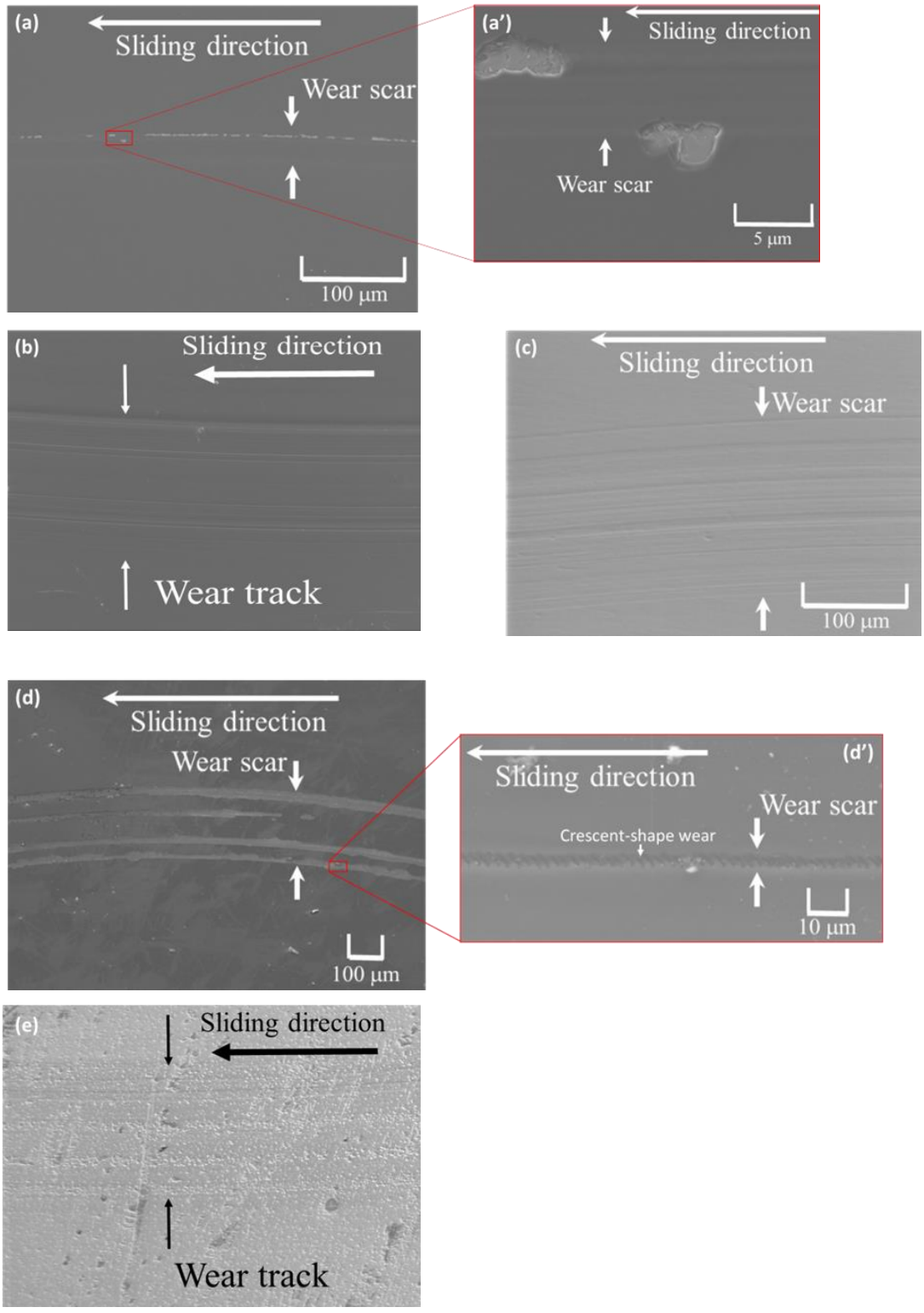

Figure 2.7 FESEM images of wear track on Si-DLC disc against SUJ2 ball under lubrication of (a) MoDTC and (a') enlargement of the surface, (b) MoO_3, (c) MoS_2, (d) Mo_2C and (d') enlargement of the surface, and (e) Mo with PAO oil

Figure 2.7 showed the effect of the 5 different particles on wear track after sliding the Si-DLC discs against SUJ2 ball, respectively. As referred to Fig. 2.7 (a), MoDTC affected the disc surface by peeling-off the Si-DLC coating due to delamination. Figure 2.7 (b) and (c) which refer to MoO_3 and MoS_2 only showed small and smooth wear track. Meanwhile, severe scratches by Mo_2C affected the coating surface as shown in Fig. 2.7 (d). Its enlargement image shows a continuous crescent-shape wear took place at the center of the peeled-off wear track. In Fig. 2.7 (e), Mo showed a presence of pit-holes-likes inside and outside of the wear track.

2.3.3 The effect of 5 different particles on the specific wear rate of a-C:H and Si-DLC disc

Figure 2.8 shows the specific wear rate of a-C:H and Si-DLC discs. At first, MoDTC which was reported as the wear acceleration material in some situation [43, 46, 65-75] showed a high specific wear rate. It is approximately 3.2 x 10^{-6} mm^3/Nm for a-C:H and 1.5 x 10^{-6} mm^3/Nm for Si-DLC. However, in the situation of Mo_2C existed in the lubricant, it showed 10 times much higher specific wear rate (approximately 3.4 x 10^{-5} mm^3/Nm for a-C:H and 3.2 x 10^{-5} mm^3/Nm for Si-DLC) compared to MoDTC.

As the research purpose mentioned above, to identify which Mo-derived compound accelerates the wear, several friction tests were conducted. As a result, Mo_2C indicated that it had the most affective wear acceleration effect rather than the others, for both DLC coatings. The high hardness of Mo_2C indicated that it had acted as an abrasive particle onto the a-C:H and Si-DLC disc as shown in Fig. 2.6 (d) and Fig. 2.7 (d), respectively.

In the case of MoS_2 and pure Mo, it was clearly shown that both materials did not enhance wear acceleration of a-C:H and Si-DLC. MoS_2 showed the lowest specific wear rate for a-C:H, approximately 0.3 x 10^{-6} mm^3/Nm and Mo also showed the lowest specific wear rate for Si-DLC, approximately 0.4 x 10^{-6} mm^3/Nm. This was proved by the FESEM images which there were no severe wear took place by MoS_2 and Mo.

MoO_3 showed higher specific wear rate approximately 1.1 x 10^{-6} mm^3/Nm rather than MoS_2 and Mo for both discs, but still three times lower than MoDTC and about 30 times much lower if compared to Mo_2C. This result indicated that Mo_2C, as the intermediate product of MoDTC, had severe abrasive effect and contributed to the highest specific wear rate of DLC for both a-C:H and Si-DLC coatings.

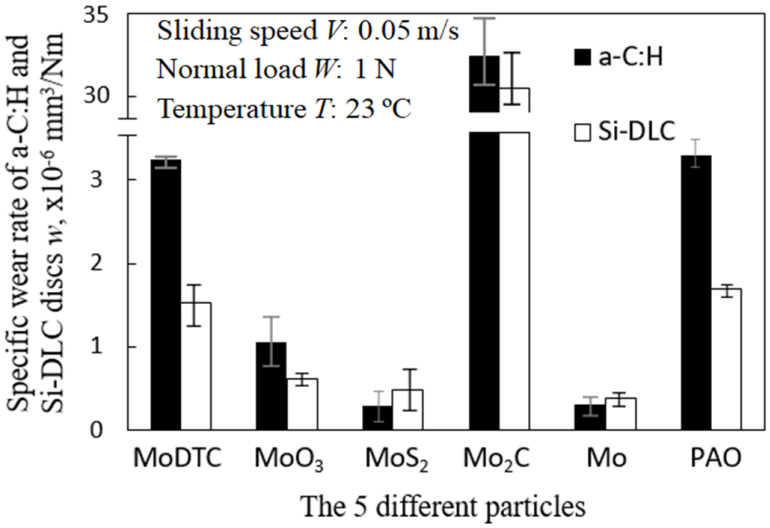

Figure 2.8 The specific wear rate of a-C:H and Si-DLC coatings against SUJ2 ball under 5 different particles contained lubrication

2.3.4 The Raman spectroscopy analysis of a-C:H and Si-DLC disc

Raman spectroscopy measurement was conducted on both inside and outside the wear track to identify graphitization and structural changes on the DLC surfaces. Raman spectra of disordered graphite consist of D-peak, approximately 1350 $cm^{-1,}$ and G-peak, approximately 1580 cm^{-1}. D-peak corresponds to the carbon disordered or defective graphitic structure. Meanwhile, G-peak features the graphitic layer and corresponds to the tangential vibration of the carbon atom. The primary characterization of graphitization is the increment of the I_D/I_G ratio and the shifting of the G-peak position [86].

The increase in intensity ratio (I_D/I_G) of the maximum disordered D-peak (I_D) intensity to the maximum graphite G-peak (I_G) intensity in the Raman spectra helps to estimate the defect density of the DLC surface. Figure 2.9 and Fig. 2.10 shows the Raman spectra and the I_D/I_G ratio inside and outside the wear track of each Mo-derived particles for a-C:H disc, respectively.

Meanwhile, Figure 2.11 and Fig. 2.12 indicates the Raman spectra and the I_D/I_G ratio inside and outside the wear track of each Mo-derived particles for Si-DLC disc, respectively. The black dotted line indicates the G-peak position of the outside wear track, and the red dotted line represents the shifted G-peak position of the inside wear track.

For a-C:H, the G-peak position of Raman spectra shifted for MoDTC and MoO_3, while the others remained at the original position. Meanwhile, there were an increment of the I_D/I_G ratio for MoDTC, MoO_3, Mo_2C and also Mo. This phenomenon indicated that graphitization and structural changes took place. Usually, when there is graphitization, the friction coefficient decreases and lead to the increment of the specific

wear rate. This was proven previously by the friction coefficient and the specific wear rate analyses on Fig. 2.5 and Fig. 2.8. However, for Mo_2C, the increment of the I_D/I_G ratio was too small.

From the view point of structural change by friction, several thousand of friction for DLC could affect structural change, although it was depend on contact pressure, speed or temperature [43, 46, 65-75]. It meant that the graphitization of DLC normally occurred gradually. Therefore, it was assumed that in the case of Mo_2C situation, those particles played a role of abrasives such as polishing to remove a gradually graphitization occurred area on the topmost surface of a-C:H coating as shown in Fig. 2.10.

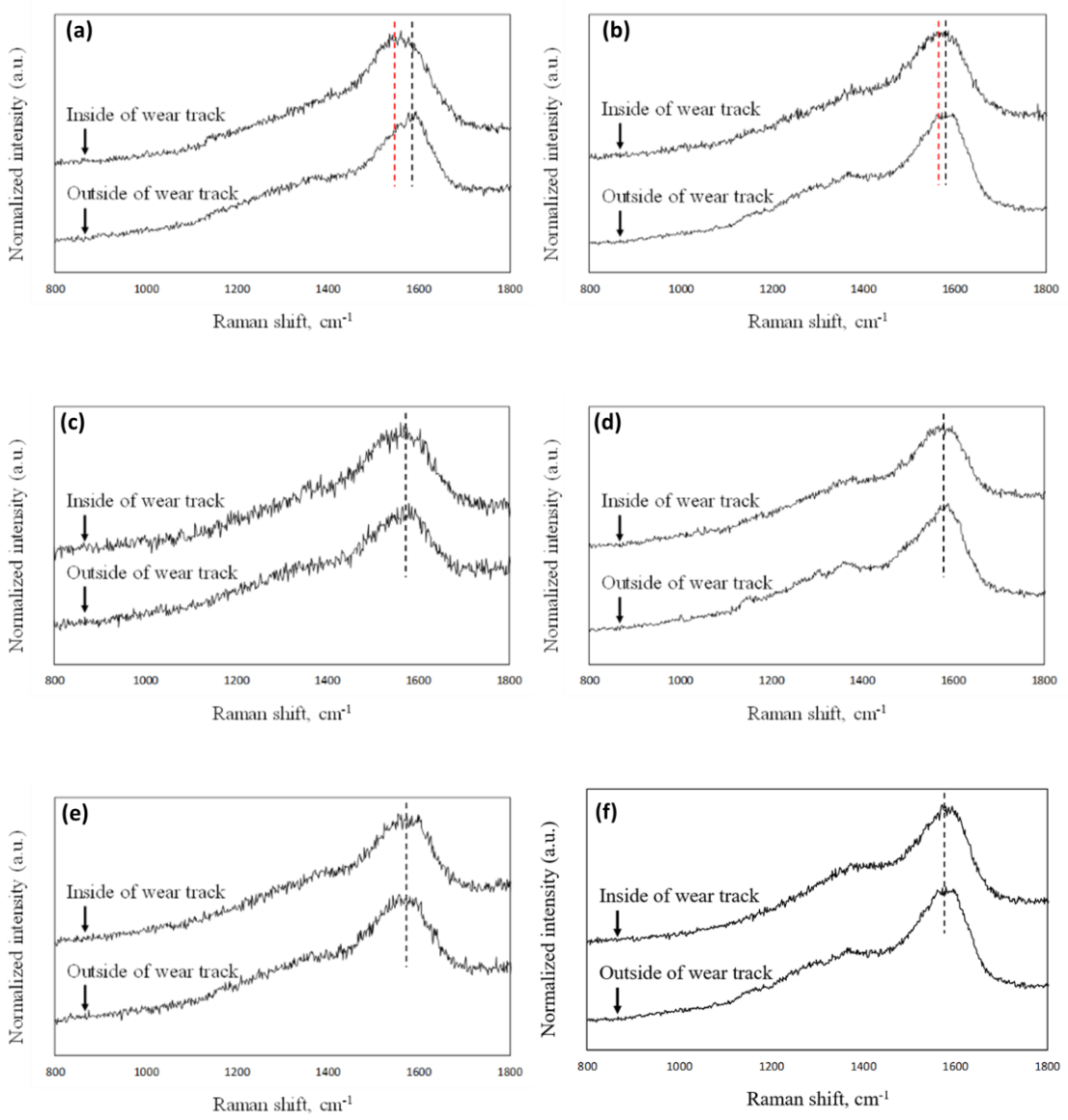

Figure 2.9 The Raman spectra inside and outside the wear track of a-C:H disc against SUJ2 ball under lubrication of (a) MoDTC, (b) MoO_3, (c) MoS_2, (d) Mo_2C, and (e) Mo with (f) PAO oil only

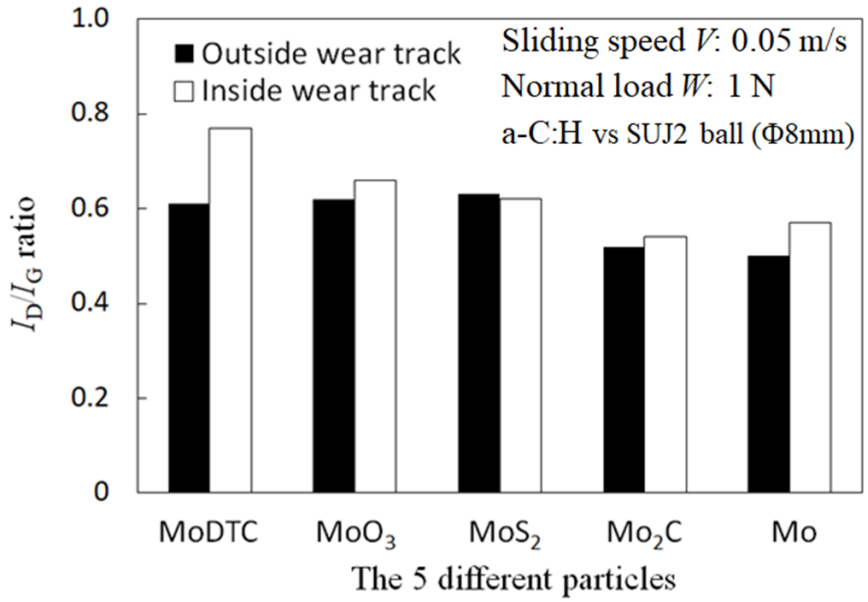

Figure 2.10 The I_D/I_G ratio of inside and outside the wear track on a-C:H coating against SUJ2 ball under 5 different particles contained lubrication

For Si-DLC, the G-peak position of Raman spectra shifted for MoDTC, MoO_3, MoS_2 and Mo_2C, while the others maintained at the original position. The slight increment of the I_D/I_G ratio took place for MoDTC and for MoS_2. However, the increment was much smaller compared to the increment for a-C:H. There were also decrements of I_D/I_G ratio for MoO_3, Mo_2C and also Mo as shown in Fig. 2.12. This results implied that graphitization by cyclic friction hardly occurred for Si-DLC.

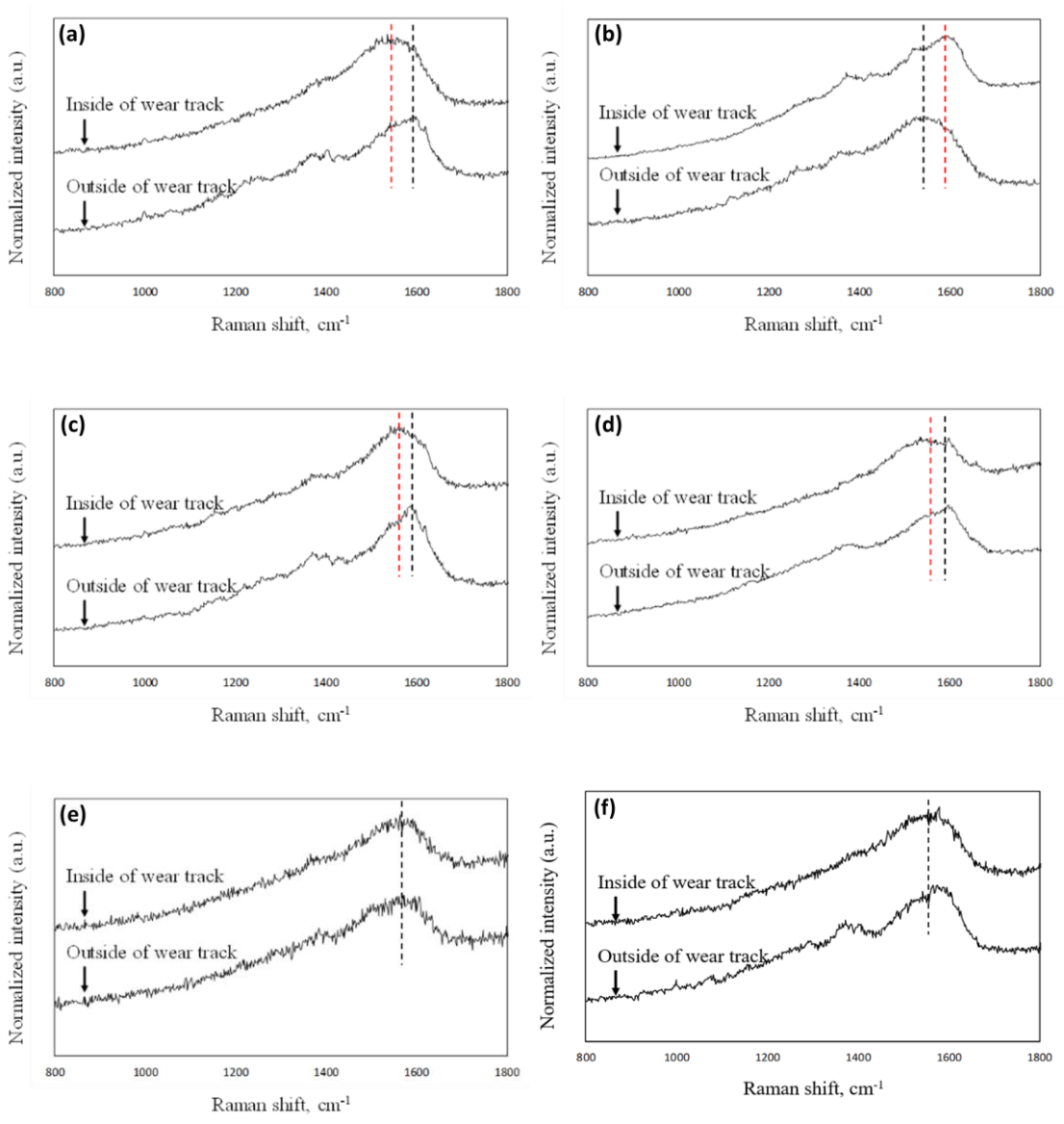

Figure 2.11 The Raman spectra inside and outside the wear track of Si-DLC disc against SUJ2 ball under lubrication of (a) MoDTC, (b) MoO_3, (c) MoS_2, (d) Mo_2C, and (e) Mo with (f) PAO oil only

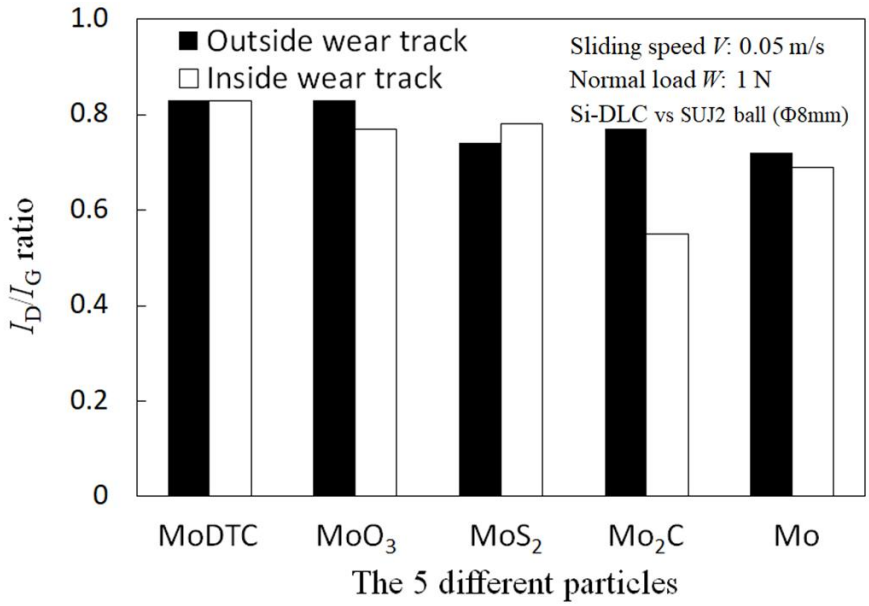

Figure 2.12 The I_D/I_G ratio of inside and outside the wear track on Si-DLC coating against SUJ2 ball under 5 different particles contained lubrication

2.4 Discussion

The use of 5 different particles is very important to understand which Mo-derived compound mainly accelerates the wear on the hydrogenated amorphous carbon DLC. The Raman analysis result of both DLC discs suggested that the structural changes effected by several Mo-derived compounds due to graphitization.

Graphitization of DLC is assumed to mainly occur because of the transformation of sp^2 from sp^3 bonding on the contact surface or generation of dangling bonds by braking up of C-C or C=C bonds. In general, carbon atoms have a tendency of making π-bond to be thermally stable. Therefore, if carbonaceous coating surface experienced some sort of chemical or mechanical reaction by additives or counterpart material, the topmost surface tend to be graphitic.

MoDTC showed that graphitization took place for both a-C:H and Si-DLC. This can be proved by the increment of the I_D/I_G ratio inside and outside of the wear track though it was too small for Si-DLC. Previous reports [59, 66-68] also stated that liquid MoDTC was degradable into another compound and reacted chemically.

In this study, powder type MoDTC was chosen to clarify the effect of itself to accelerate wear of a-C:H and Si-DLC because of those particles were assumed to have less contacting occasions to the surface without a Hertzian contact zone rather than liquid type additives. Therefore, the MoDTC particles was able to affect wear acceleration only at the contact zone when it entered between SUJ2 ball and a-C:H coating.

During the direct contact of those particles between the SUJ2 ball and a-C:H coating, based on the hardness of MoDTC (1.0 GPa), it was impossible for MoDTC particles to accelerate the wear as abrasive since the hardness of a-C:H (18 GPa) and Si-DLC (25 GPa). That impossibility of wear acceleration by hardness order implied fact MoDTC might have a role to accelerate wear of a-C:H by chemical assistance without mechanical effect.

For Si-DLC, the coating was peeled-off by delamination from the topmost surface without whole peeling off from the interface. However, no such kind of crescent-shape wear took place since the Si-DLC is harder than the a-C:H and the Si-doped coating had not been removed during the friction test. Thus, powder-type MoDTC also reacted chemically to accelerate the wear on a-C:H and Si-DLC.

According to the MoO_3 in lubrication, the specific wear rate as shown in Fig. 2.8 indicated that MoO_3 have affection to accelerate wear as catalytic effect from the view point of hardness. The I_D/I_G ratio of a-C:H increases by MoO_3 assumed to be caused by oxidization to promote structural changes or making covalent bonds between

a carbon and oxygen atom, and reducing the hardness of a-C:H coating simultaneously. On the other hand, MoO_3 has no synergistic effect on a Si-DLC surface, thus less wear rate was obtained.

MoS_2 has the lowest specific wear rate for a-C:H and second lowest for Si-DLC. MoS_2 which is well-known as a solid lubricant formed a protective layer on the DLC surface, covering the asperity tips and reducing the wear rate. This was also supported by the findings in [70-71] which stated that MoS_2 promoted tribofilm formation to give good wear resistant ability. MoS_2 coating was also functioned as additive source to the lubricating oil as reported in [98]. Therefore, MoS_2 was incapable to support wear acceleration material from the MoDTC degradation.

Mo_2C showed the highest wear rate for both a-C:H and Si-DLC coatings. From the Raman analysis, it was hard to conclude that graphitization clearly occurred on the a-C:H disc because of the I_D/I_G ratio did not change significantly. Its wear effect was assumed to mainly due to the repetitive rubbing that continuously having gradual removal of surface coating during the friction test. This phenomenon was explained by the layers of flaky structure peeled-off from the coating as shown in Fig. 2.6 (d).

For Si-DLC, the rubbing repetition of Mo_2C particles continuously removes the coating and a continuous crescent-shape wear was formed at the center of the peeled-off wear track. Based on the wear track image in Fig. 2.7 (d), the surface had damaged by Mo_2C particles as abrasive wear and the surface was experienced shallow peeling without cyclic friction. This is related to the significant decrement of the I_D/I_G ratio. Normally, DLC showed graphitization by cyclic friction, but, in Mo_2C case, graphitization did not occur. So, a sample of depth analysis was conducted on a-C:H, by using a Calotester to make a dent and measure the surface at different depth of the coating by surface-enhanced Raman spectroscopy, which will be further discussed in

Chapter 3. The hydrogen content increased with the depth from the interface of the Si-DLC to the substrate. It indicated that along the depth, the coating showed higher sp^3 content rather than the topmost surface. The as-deposited a-CH and Si-DLC showed the depth distribution of sp^2 and sp^3, and the topmost layer is sp^2 rich. After severe abrasive wear on Si-DLC which removed the topmost surface of the coatings, the surface after the friction test was sp^3 rich. Thus, it can be concluded that Mo_2C was the main by-product from MoDTC degradation that promotes the wear acceleration abrasively.

Finally in the situation of Mo existed in lubrication, the Raman analysis showed that there was a structural change on the a-C:H disc from the increment of the I_D/I_G ratio. However, the observation of the wear effect on the surface was not severe, plus its specific wear rate maintained at the lowest value. The wear process of Mo existing was almost same tendency with MoS_2. For Si-DLC, no structural changes occurred from the viewpoint of I_D/I_G ratio value and the wear rate remained at the lowest value.

However, its FESEM image revealed there was pit-holes dents inside and outside of the wear track. Those surface dents were generated on the a-C:H surface without friction effect. Probably, Mo had a possibility to react as catalyst to the Si-DLC, then it was suggested to enhance carbon atoms or C-H bonds detachment from a-C:H surface. Eventually, pit-holes dents were left on the surface. Since Mo which was a pure compound had little significant effect on the wear acceleration, it is neglected as the wear acceleration material from the MoDTC degradation.

The comprehensive reactions of the 5 different particles on the a-C:H are summarized in Fig. 2.13 and the sequence of reactions are based on a literature [46]. At first, the MoDTC itself accelerates wear of a-C:H by catalytic effect and changes the

structure of a-C:H. Then, degrades to form intermediate material of MoS_2 [46]. However, this intermediate material does not contribute to the wear acceleration. The other intermediate material, MoO_3 are generated from MoS_2 is able to enhance wear acceleration rather than MoS_2.

Eventually, Mo_2C are generated from MoO_3 shows a significant effect on the wear acceleration. The specific wear rate escalates 10 times higher than the MoDTC. Due to its high hardness properties, the Mo_2C scratches the a-C:H surface abrasively. This acknowledges that Mo_2C is the main contributor to the wear acceleration from the degradation of MoDTC. Nonetheless, with the inclusion of Silicon-doped onto the a-C:H, it prevents the structural changes from taking place and does reduce the wear effect on the DLC surface.

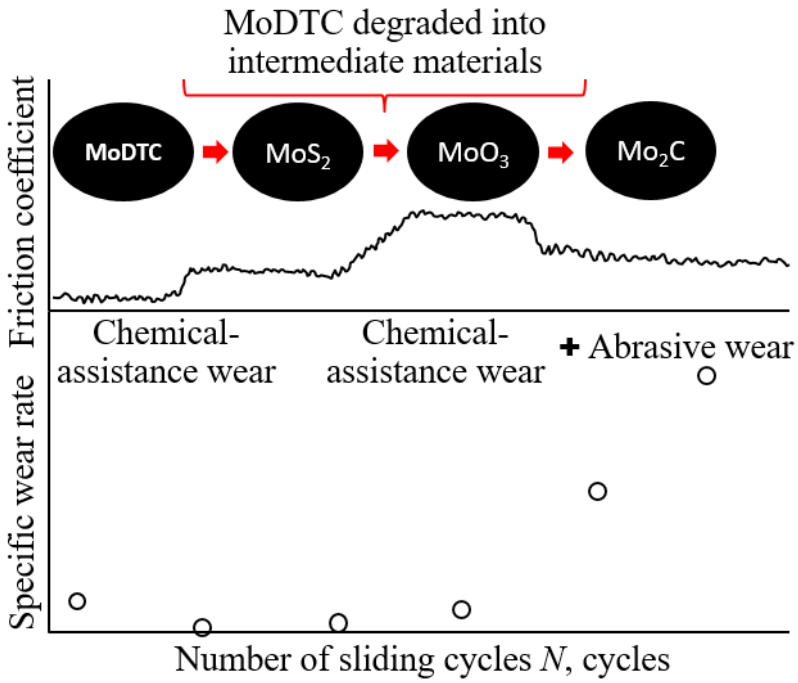

Figure 2.13 Summary of 5 different particles effect on wear behaviour of a-C:H

2.5 Conclusion

In this study, the friction and wear of the hydrogenated amorphous carbon (a-C:H) against SUJ2 ball under PAO lubrication with/without Mo-derived particles into the oil under boundary lubrication at room temperature were conducted to have well understanding about the effect of degradation of MoDTC during friction.

To solve the problem, five types of Mo-derived particles; MoDTC, MoS_2, MoO_3, Mo_2C, and, Mo were prepared and conducted short friction tests such as 1500 cycles. a-C:H and Silicon-doped a-C:H (Si-DLC) were prepared to analyze the tribological effects. The material properties differences of those two DLC coatings resulted in divergent of the tribological effect by the 5 different particles. From the tribological analysis, it can be concluded as follows:

- The specific wear rate of a-C:H and Si-DLC under MoDTC existed in PAO oil showed 3.2 x 10^{-6} mm^3/Nm for a-C:H and 1.5 x 10^{-6} mm^3/Nm for Si-DLC. On the other hand, in the case of Mo_2C in PAO oil, the specific wear rate of a-C:H was the highest approximately 3.4 x 10^{-5} mm^3/Nm for a-C:H and 3.2 x 10^{-5} mm^3/Nm for Si-DLC. MoO_3 showed higher specific wear rate approximately 1.1 x 10^{-6} mm^3/Nm rather than MoS_2 and Mo (both were approximately same as 0.3 x 10^{-6} mm^3/Nm for a-C:H and 0.4 x 10^{-6} mm^3/Nm for Si-DLC) for both discs. Therefore, Mo_2C from MoDTC degradation was the major contributor to the wear acceleration.

- According to the MoO_3 in lubrication, the specific wear rate indicated that MoO_3 have affection to accelerate wear as catalytic effect from the view point of hardness. Based on the hardness of MoDTC (1.0 GPa), it was impossible for MoDTC particles to accelerate the wear as abrasive since the hardness of a-C:H (18 GPa) and Si-DLC (25 GPa). That impossibility of wear acceleration by hardness order implied fact that MoDTC might have a role to accelerate wear of a-C:H by chemical assistance without mechanical effect.

Chapter 3

Wear Acceleration of a-C:H Coatings by Molybdenum-derived Particles: Mixing and Temperature Effects

3.1 Introduction

In the modern automotive world, electric or hybrid-type vehicles are currently the most popular lineup for customers because of peoples' awareness of environmental friendliness, the need to reduce harmful chemical waste from exhaust gases, and the need for low energy consumption. However, most automotive manufacturers continue to manufacture internal combustion engine automobiles [99]. Therefore, reducing the frictional force and heat generated at piston rings and liners in an engine cylinder remain important research targets [100]. There have been several approaches to understanding the acceleration of wear of diamond-like carbon (DLC) by solid particles [101-103] and lubricant additives [43, 46, 65-75]. However, degradation of the lubricating ability of those additives has prevented a better understanding of wear acceleration itself [46].

Previously in Chapter 2, the effects of degradable materials delivered from molybdenum dithiocarbamate (MoDTC) on accelerating the wear of hydrogenated amorphous carbon (a-C:H) and silicon doped hydrogenated amorphous carbon at room temperature have been reported [104]. The powder-type MoDTC showed a greater

ability to accelerate wear than molybdenum trioxide (MoO_3), regardless of the hardness of those particles. Of course, molybdenum carbide (Mo_2C)—which has the highest hardness among pure Mo, MoO_3, MoDTC, and molybdenum disulfide (MoS_2)—has a major role in enhancing wear because of its hardness, which makes it useful as abrasives in the polishing field [65].

MoDTC has been reported to be an easily degradable compound, and it tends to change its physical and chemical structure [46]. Previous investigations assumed that intermediate products from the degradation of liquid MoDTC accelerated the wear of DLC [68]. Mo-derived compounds such as MoS_2 and MoO_3 have also been reported to form tribo-layers on hydrogenated DLC and promote chemical wear. The other Mo-derived compound, Mo_2C, has also been found to cause abrasive wear on DLC surfaces [66-68, 104].

Many conclusions and assumptions have been made. For example, Al-Jeboori et al. reported that using cast iron for friction tests against a-C:H under a fully formulated lubricant containing MoDTC resulted in no MoO_3 formation during friction tests [105]. From a series of studies, they reported one possible wear mechanism of a-C:H from a lubricant containing MoDTC: that MoS_2 formed by the degradation of MoDTC due to reactions with the C–H bond and the cutting of the covalent bond [106]. Okubo et al. [107] reported *in-situ* Raman observations of a-C:H against an AISI 52100 bearing steel ball under fully formulated 0W-20 oil, in the grading scheme of the American Petroleum Institute (API). Their results indicated that oil containing MoDTC had been degraded under friction between the a-C:H and the AISI 52100 steel and that a phosphate-related anti-wear additive had formed a thick tribo-layer on the steel surface, with MoS_2 at the topmost surface of the layer. This produced a “no wear” a-C:H coating. Okubo et al. concluded that the “high wear” was due to the formation of

Mo_2C [107].

The acceleration of the wear of a-C:H related to the MoDTC degradation was assumed to be strongly affected by the main kind of Mo-material formed during friction. Although some Mo compound certainly accelerates the wear, whether it is MoDTC itself or one or more of the compounds derived from MoDTC degradation is still unknown. Thus, it is essential to identify which Mo-derived compound plays a major role in enhancing wear under real engine conditions.

Normally, Raman analysis gives information about the surface of material within several hundred nanometers from the topmost surface, but such analysis yields only a little information about the actual surface while it provides more information about the deeper parts of the surface layers (i.e., the bulk interior). If it is possible to acquire information about only the topmost surface to undertake comparisons among a-C:H surfaces that have experienced friction tests with various Mo-related materials, it is expected to be able to classify the frictional effects of Mo-related materials as abrasive, oxidation, or chemical reactions. Therefore, surface-enhanced Raman scattering (SERS) procedure is introduced in this chapter. SERS analysis is highly capable to obtain Raman data only at the topmost surface, less than 2 nm depth.

At room temperature and under boundary lubrication, Mo_2C powders had the abrasive effect of scratching the a-C:H surface as hard particles, while MoO_3 powders accelerated wear by a catalytic effect as reported in Chapter 2 [104]. However, it remained unclear whether those particles caused enhanced wear of a-C:H in a poly alpha-olefin base oil at 80ºC, which is generally thought to be the normal operating temperature of a combustion engine. The main purpose of this chapter is to clarify the mechanism that is responsible for the wear acceleration effect of Mo-related materials at 80ºC, using the SERS analysis to obtain information at the topmost surface of a-C:H.

3.2 Experimental Procedure for Friction Tests, Preparation of Oil with Powders, and Analysis using Field-emission Scanning Electron Microscopy (FE-SEM) and Surface-enhanced Raman (SERS)

Ball-on-disc friction tests were conducted under boundary lubrication conditions with several different Mo-derived powders at 80°C. The experimental setup is shown schematically in Fig. 3.1 (a) as a front view and (b) as a top view. The upper-side mating material was high-carbon chromium-bearing steel (SUJ2) ball with a diameter of approximately 8.0 mm, and it was pressed against an a-C:H coated disc. The a-C:H was coated onto a silicon-wafer [Si (100)] substrate using chemical vapor deposition. The a-C:H coating was submerged in an oil bath consisting of a mixture of base oil and one of five different types of particles. The oil bath was connected to a rotary shaft, and it was equipped with a heater and a thermocouple inside the rotating part. Particles were dispersed into base oil (PAO) with a viscosity of 19.0 mm^2/s for this study. The powder mixture was heated to 80°C to identify the effect of the oil temperature on the a-C:H wear. Before starting the friction test, each mixture of base oil with one of the five different types was stirred in an ultrasonic bath for one hour to reduce particle settlement and prevent unbalanced mixtures. Each test was conducted for 1500 cycles in 10 minutes at a speed of 0.05 m/s at 80°C under an applied load of 1.0 N, which corresponds to a maximum initial Hertzian contact pressure of 455 MPa.

The a-C:H undergoes a nano-indentation test (Elionix, ENT-1100a) to determine the coating hardness, which was approximately 13.0 GPa. To quantify the roughness, atomic force microscopy (AFM) measurements (SPM-9700HT) were conducted. The a-C:H had an arithmetic surface roughness R_a = 1.0 nm, and the coating thickness was approximately 0.5 μm.

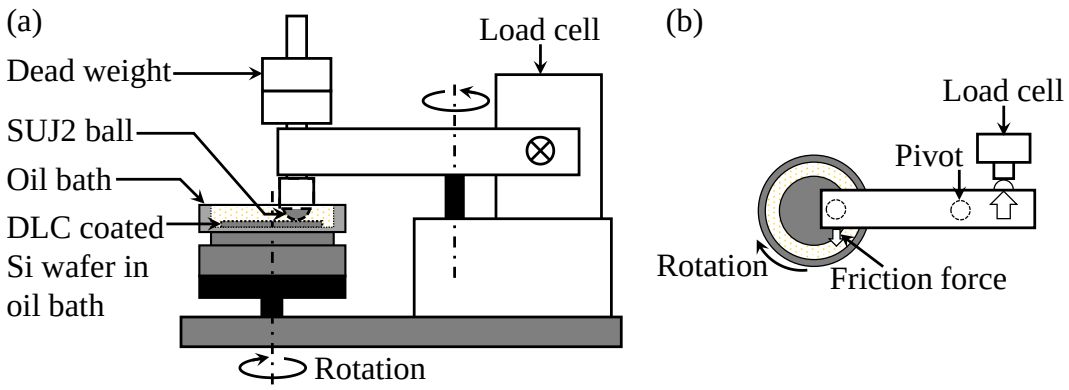

Figure 3.1 Schematic illustration of the ball-on-disc tibometer.

(a) Front view and (b) top view

The five different types of particles—MoDTC, MoS_2, Mo, MoO_3, and Mo_2C—had sizes between 2.0 and 5.0 μm, and were dispersed into the base oil at 0.1% by volume. The particle hardness were ordered as follows: MoDTC (1.0 GPa), MoS_2 (1.0 GPa), Mo (1.5 GPa), MoO_3 (2.5 GPa), and Mo_2C (15 GPa). Except for MoO_3, all the particles were procured from the same material supplier. The MoO_3 particles were synthesized experimentally from MoS_2 in the laboratory [104].

To eliminate oil stains and contaminants, each sample was cleaned with benzene and then acetone in an ultrasonic bath both before and after the friction test. The wear of the a-C:H discs were observed by using both an optical microscope and FESEM. Then, the a-C:H discs were analyzed using Raman spectroscopy (Jasco, NRS1000; the probe diameter was approximately 2 μm) under 532-nm wavelength irradiation, with a 10 mW output beam covering the range 800–1800 cm^{-1} to obtain both the normal Raman and the SERS results.

Since the normal Raman wavelength can penetrate through the coating surface to depth of several hundred nanometers to micrometers, the final result is affected by the deeper layers. Therefore, the SERS procedure was introduced to obtain information about the topmost surface only [88]. Experimentally, a portion of the wear track on the a-C:H disc was covered with a 0.1 μL droplet containing a mixture of gold nanoparticles (AuNPs). The AuNPs were allowed to dry before undertaking the Raman analysis. Before measuring the Raman spectra of the sample, several indentation marks were applied using a diamond indenter to enable recognize the measurement position. These procedures are shown in Fig. 3.2.

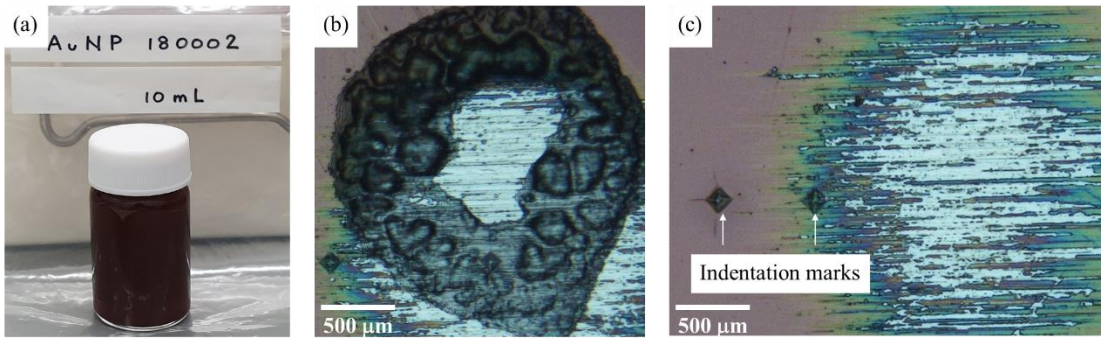

Figure 3.2 Sample preparation for SERS. (a) AuNPs. (b) The AuNPs are drying out few minutes after applied. (c) The indentation marks at sample surface.

After that, the a-C surface was measured using normal Raman analysis, then the AuNPs were added onto the surface, and finally re-analyzed at the same measurement position. The depth resolution of the SERS analysis was confirmed prior to this research. Figure 3.3 shows a schematic illustration of the application of the AuNPs onto a confirmation sample of amorphous carbon (a-C) coating approximately 1.7 nm thick on a Si(100) substrate [88]. Figure 3.4 shows the representative result. The results showed that only SERS analysis did not detect the Si (100) substrate at around 900–1000 cm^{-1}. Thus, the SERS analysis included at most 2 nm below the topmost surface.

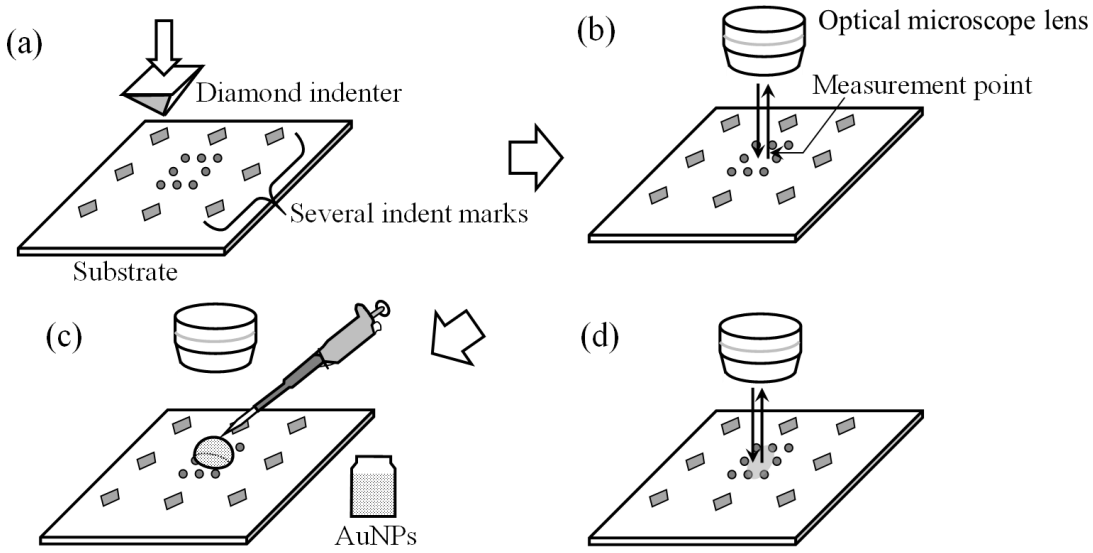

Figure 3.3 Schematics illustration of the application of AuNPs onto a specimen. (a) Placing several indentation marks on the specimen using a micro-Vickers hardness tester and nano-indentation tester. (b) Normal Raman analysis for a measurement point using an optical microscope. (c) Applying AuNPs in a liquid droplet after normal Raman analysis. (d) SERS analysis conducted at the same position as in (b)

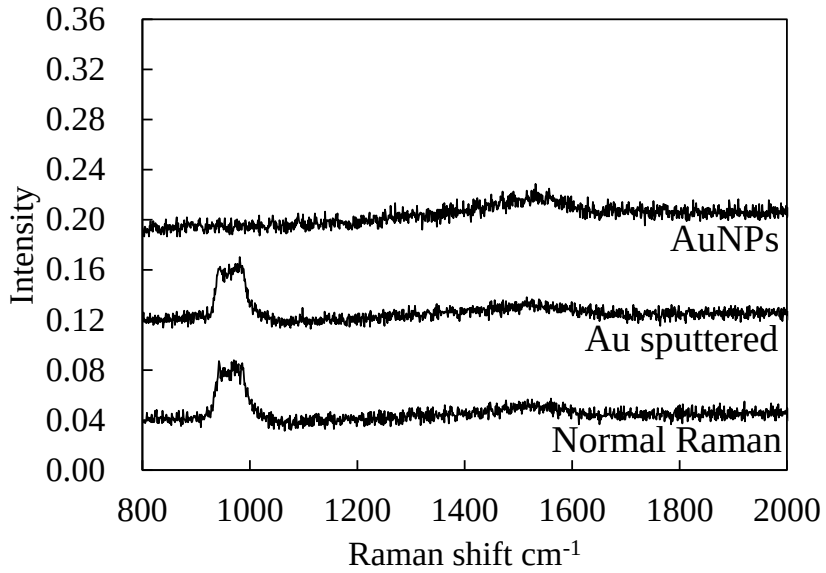

Figure 3.4 Representative data comparing the SERS analysis (labelled “AuNPs” and “Au sputtered”) and normal Raman analysis [107]

Representative SERS analyses for a-C:H at different depths have been reported before in the same laboratory [88]. The surface with a "Calotester" was shaped into a spherical dent so that it was possible to measure different positions in the plane as different depths from the topmost surface to the interface between the a-C:H coating and the Si substrate.

The hydrogen concentration was then calculated from the slope of Raman baseline "m" and the peak graphite intensity I_G, which is assumed to be related to the hydrogen content in that a-C:H coatings [109]. The hydrogen concentration was calculated from the following equation given by [109];

$$H\ [at.\%] = 21.7 + 16.6 \log\{m/I_G\ [\mu m]\} \qquad (3.1)$$

Figure 3.5 shows the relation between the SERS results and the distance of the topmost surface from the interface between the a-C:H coating and the silicon substrate. The topmost surface is approximately 3800 nm above the interface. The hydrogen concentration increases gradually with the thickness of the coating above the interface. The height measurement was conducted using the Calotester to make a dent, then the AuNPs was dispersed on the sample. Under the Raman analysis equipment, the position of Calotester dent which related to the depth of coating is chosen by using XY-stage. The AuNPs SERS analysis is capable to obtain within 1.7 nm or less depth of each measurement point [88].

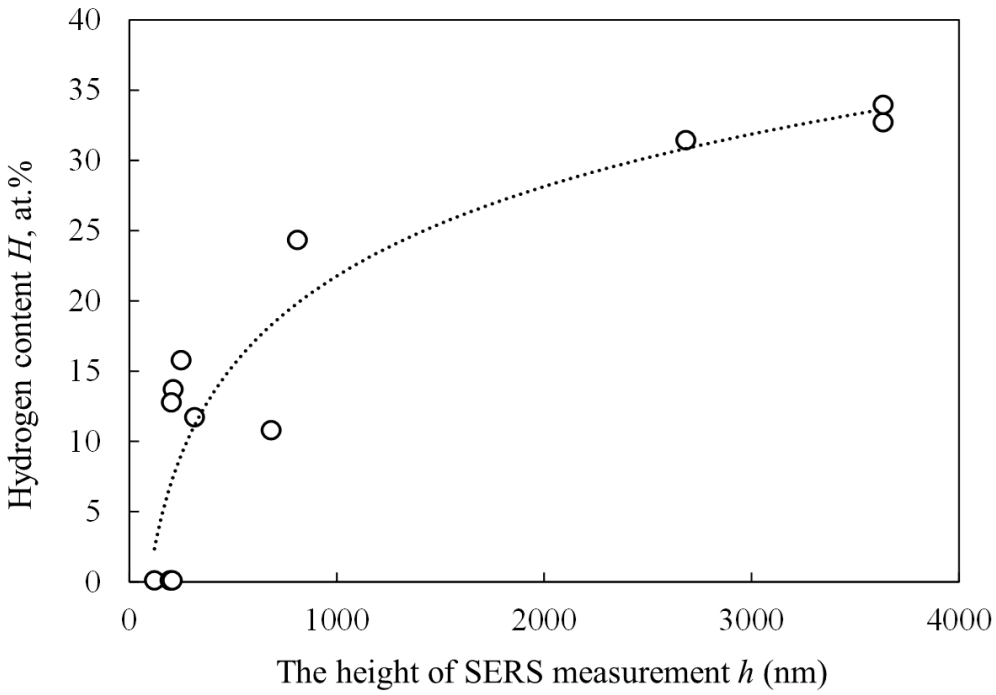

Figure 3.5 Hydrogen concentration at each depth in an a-C:H coating from the interface between the a-C:H coating and the Si substrate

3.3 Results

3.3.1 Friction coefficient of the a-C:H disc at 80°C for several Mo-related particles

Friction tests were conducted at 80℃ with or without several Mo-related particles under boundary lubrication conditions. A representative result of the frictional behaviour is shown in Fig. 3.6 (a) for the PAO lubricant with Mo_2C powder, and Fig. 3.6 (b) shows a plot of the average friction coefficient from the beginning to the end of the friction test for each powder.

The friction coefficient fluctuates from cycle to cycle, but all the friction tests also showed similar fluctuations in the value of the friction coefficient. The average friction coefficients are plotted in Fig. 3.6 (b) as a function of particle hardness.

The effective hardness of the mixture of Mo_2C, MoO_3, and Mo was assumed to be the average of their separate hardness. These results show that Mo and the particle mixture were the most effective in increasing the friction coefficient, which approximately 0.12.

Both MoO_3 and MoS_2 showed almost the same lowest value, approximately 0.087. MoDTC, Mo_2C, and PAO had intermediate friction coefficients of approximately 0.09 and 0.11, respectively. However, although MoDTC is a well-known friction modifier, it did not function effectively at 80°C to maintain the friction coefficient at the lowest level.

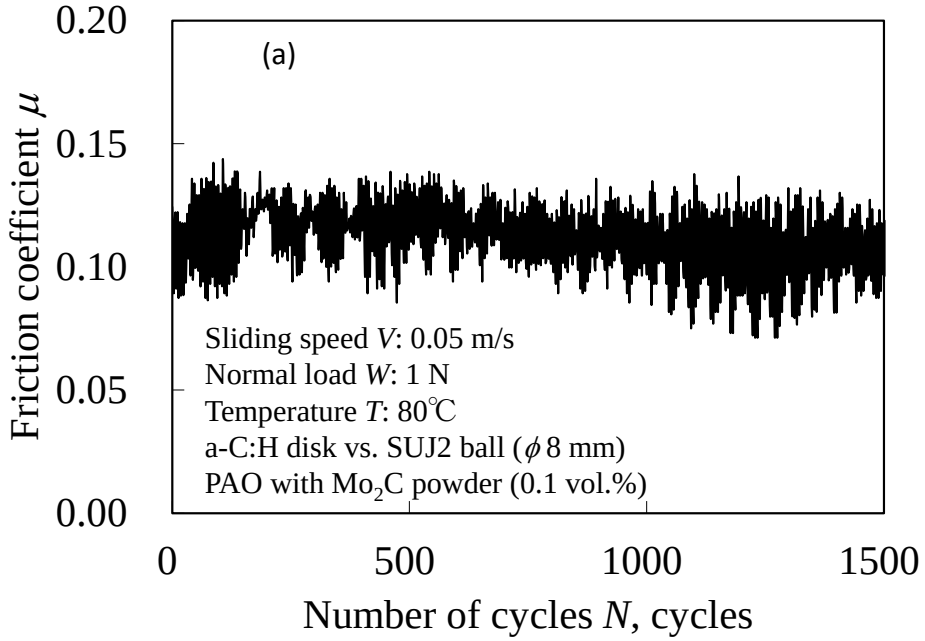

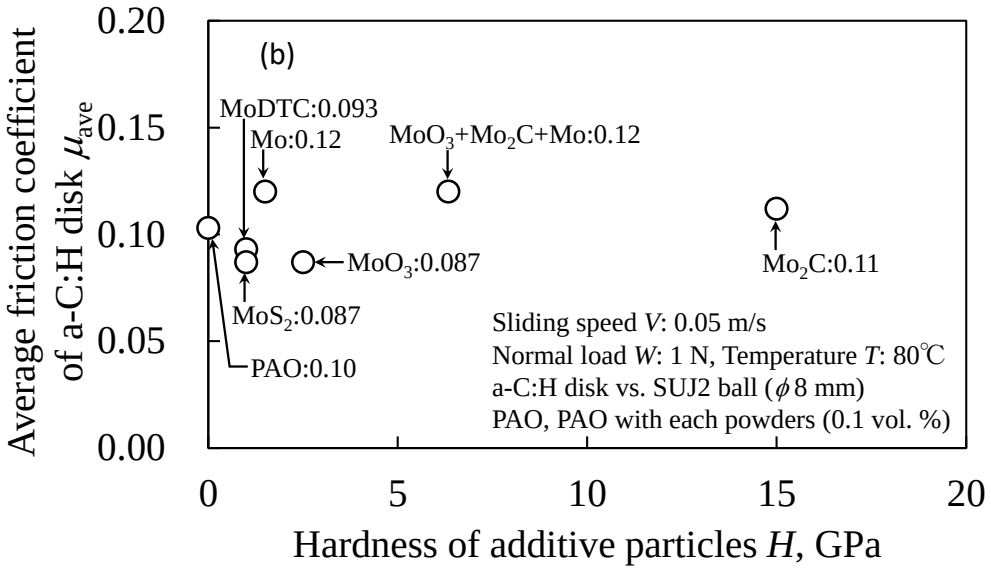

Figure 3.6 (a) Representative data showing the friction coefficient of particles dispersed into a base oil (PAO) with Mo_2C as a function of the number of cycles. (b) The average friction coefficients of a-C:H under boundary lubrication conditions at 80°C as a function of particle hardness

3.3.2 Optical-Microscope and AFM observations of wear tracks on a-C:H discs and the specific wear rate

After the friction tests, the a-C:H discs were observed under an optical microscope, as shown in Fig. 3.7 (a)–(f), and the specific wear rates were calculated from cross-sectional information obtained with a laser microscope, as depict in Fig. 3.8). For both Mo_2C and the particle mixture, the surface had severe scratch marks, as shown in Fig. 3.7 (d) and (f). Referring to Fig. 3.5, these two types of particles are the hardest among those considered here.

From a Hertzian contact calculation, the diameter of the contact area is expected to be approximately 60 μm. The wear tracks for MoDTC, MoO_3, MoS_2, and Mo are all in the same group without severe scratches. The outside of the wear track for Mo_2C showed many scratch marks. It is assumed that this occurred because Mo_2C particles got caught between the SUJ2 ball and the a-C:H coating and that the powders scratched the surface as abrasives.

Figure 3.8 shows the specific wear rate w of the a-C:H discs as a function of the hardness of the additive particles at 80°C, with some 23°C data added for comparison with the 80°C data. Without Mo-related particles, the specific wear rate was very small, such as at the order of 3.5×10^{-6} mm^3/Nm. MoS_2, which is a prominent solid lubricant, showed the lowest specific wear rate, $w = 3.0 \times 10^{-6}$ mm^3/Nm. Additionally, MoDTC and Mo showed almost the same low specific wear rates, approximately 7.9×10^{-6} mm^3/Nm, and 8.1×10^{-6} mm^3/Nm, respectively. This is probably related to the hardness of the particles which are both around 1.0–1.5 GPa. The low hardness did not produce a significant increase in the specific wear rate, either chemically or mechanically, at high temperature. However, the specific wear rate of MoO_3, 25.7×10^{-6} mm^3/Nm, was

very surprising, since it also had a low hardness (2.5 GPa). Therefore, the specific wear rate of 3.1×10^{-6} mm^3/Nm at 23°C as obtained in [73] was added for comparison. This shows that the specific wear rate increased by about a factor of eight. This shows that the increased temperature increases the specific wear rate of MoO_3, regardless of the hardness of these particles.

After the friction test of 23°C with MoO_3, one MoO_3 particle was fortunately observed on the a-C:H coating as shown in Fig. 3.9. The SEM observation clearly showed MoO_3 particle on the a-C:H coating as shown in Fig. 3.9 (a) and the enlargement image of (b). The energy dispersive spectroscopy (EDS) images of molybdenum are shown in (c) and oxygen is shown in (d). In Fig 3.10 (b) showed the area coloured grey between the white-dotted line looks wedge generated by ploughing effect. Figures 3.10 (c) and (d) clearly exhibited that the area did not include molybdenum and oxygen. This result clearly indicated that MoO_3 did not diffuse to a-C:H surface during the friction test.

The specific wear rate of Mo_2C, 58×10^{-6} mm^3/Nm, was the highest of all the particles. It is also compared with the result at 23°C from [78], which was around 34×10^{-6} mm^3/Nm. The wear rate increased by less than a factor of two, showing that the abrasive Mo_2C particles were less affected by temperature than MoO_3. The particle mixture MoO_3+Mo_2C+Mo displayed a high specific wear rate of 50×10^{-6} mm^3/Nm. This was less than the wear rate for Mo_2C but around twice as high as that of MoO_3.

After the friction tests, the a-C:H surfaces were observed using AFM. Those results are shown in Fig. 3.10. The surfaces were damaged by several scratch marks in the same direction as in the friction tests.

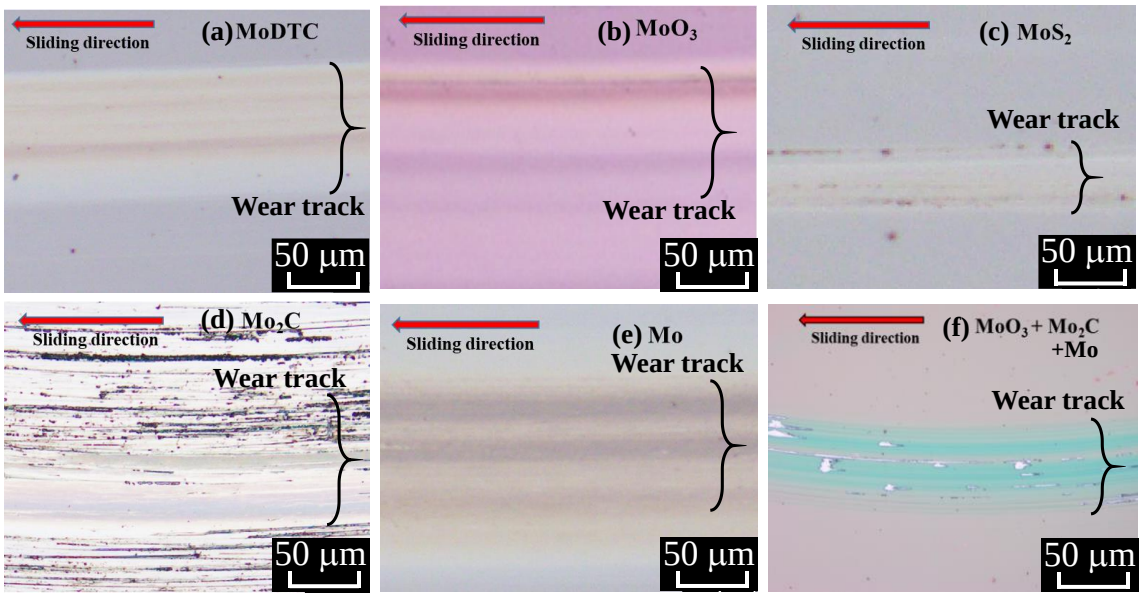

Figure 3.7 Optical-microscope images of a-C:H discs after the friction tests. (a) MoDTC, (b) MoO_3, (c) MoS_2, (d) Mo_2C, (e) pure Mo, and (f) the MoO_3+Mo_2C+Mo mixture

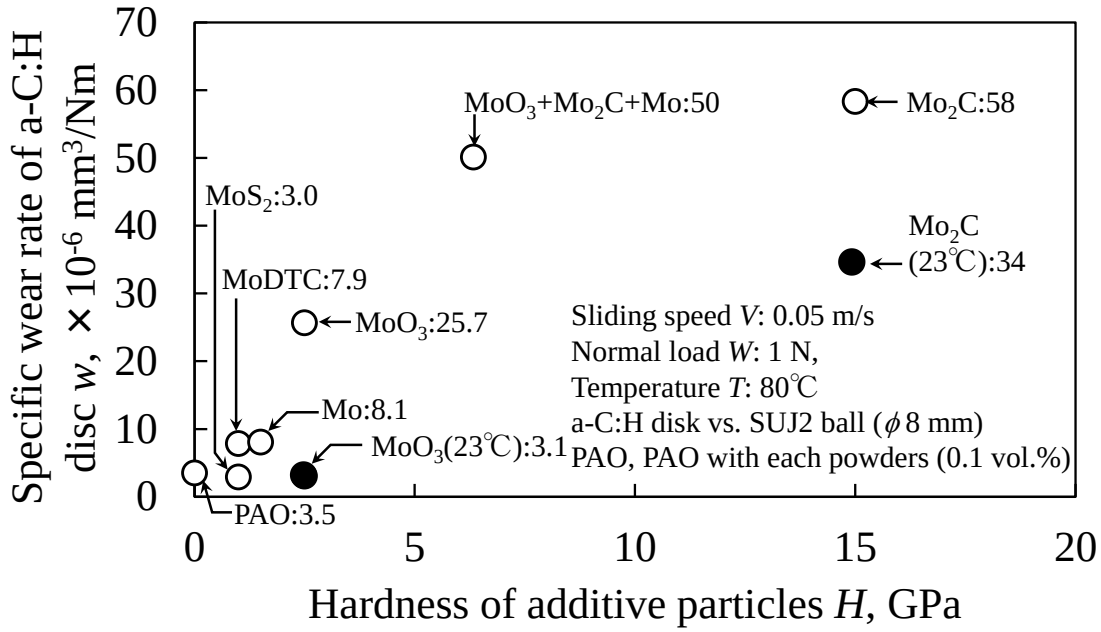

Figure 3.8 The specific wear rate w of a-C:H discs under several lubrication. The values for MoO_3 and Mo_2C at 23°C were obtained from the previous data [37]

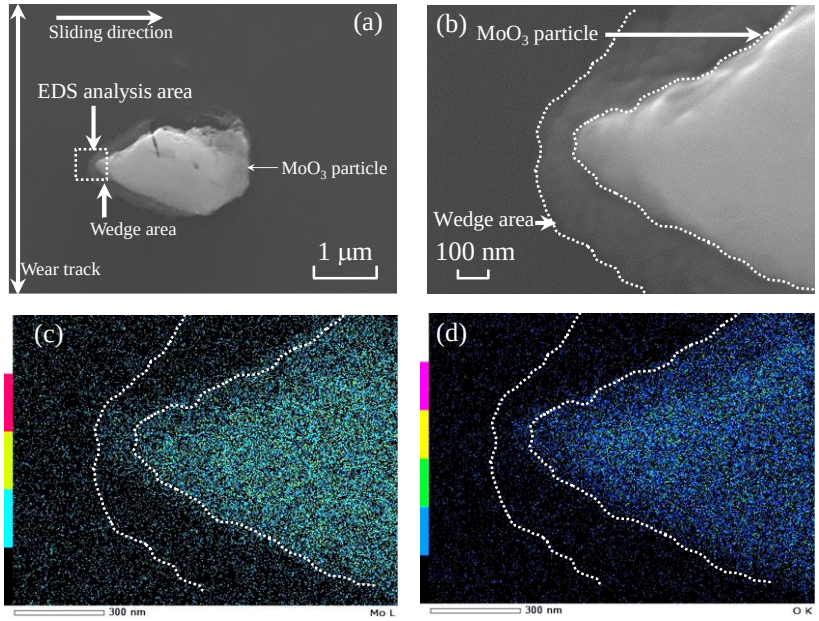

Figure 3.9 (a) The SEM observation of a MoO_3 particle on the a-C:H wear track. (b) Enlargement of the MoO_3 particle indicated in (a) as white-dotted square. (c) EDS mapping result of molybdenum. (d) EDS mapping result of oxygen

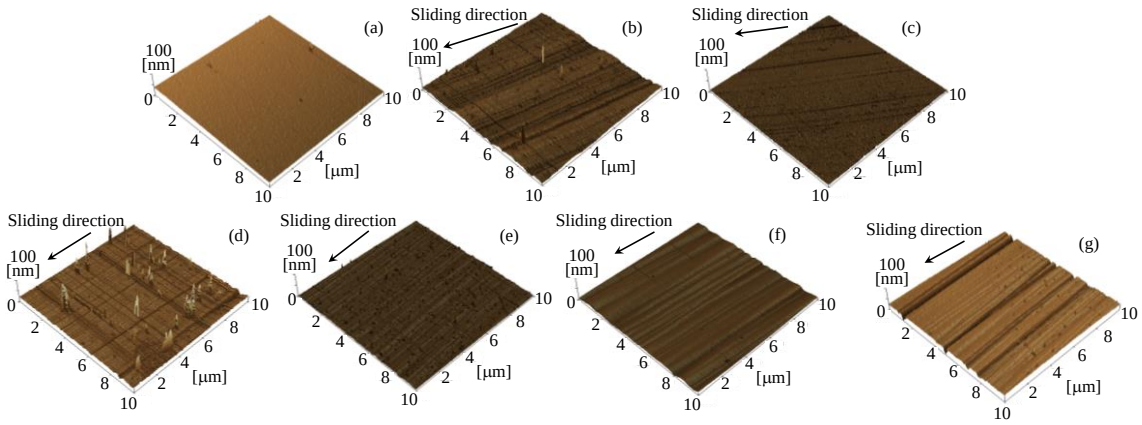

Figure 3.10. Surface roughness observations by AFM in the wear scars of the a-C:H discs. (a) The as-deposited a-C:H surface: 0.3 nmRa, 70 nmRz. (b) MoO_3: 2.6 nmRa, 94 nmRz. (c) MoS_2: 0.8 nmRa, 39 nmRz. (d) Mo_2C: 1.8 nmRa, 165 nmRz. (e) Mo: 0.8 nmRa, 52 nmRz. (f) MoDTC: 1.4 nmRa, 35 nmRz. (g) MoO_3+Mo_2C +Mo mixture: 3.4 nmRa, 60 nmRz.

For both (c) MoS_2 and (e) Mo, the maximum surface roughness decreased from that of the as-deposited one. Both (b) MoO_3 and (d) Mo_2C showed higher maximum surface roughness than the as-deposited one. Finally, the particle mixture (g) showed several deep scratch marks, even though, the maximum surface roughness was comparable to that of the as-deposited surface.

3.3.3 Normal Raman and SERS analyses for the a-C:H discs at the topmost surface of the wear tracks and for the as-deposited surface

The fundamental characterization of graphitization is provided by the increase in the I_D/I_G ratio and the shift in the position of the G-peak. To identify the defect density of the a-C:H surface, the intensity ratio (I_D/I_G) of the maximum disordered D-peak intensity I_D to the maximum graphite G-peak intensity I_G from the Raman spectra was measured [86]. The SERS measurements provided the best option for obtaining more accurate results.

Figures 3.12 (a) and (b) show representative data for an a-C:H coating analyzed by normal Raman spectroscopy for the outside and inside of the wear track, respectively, and Fig. 3.11 (c) shows the SERS results after the friction test with the MoO_3 powder, as representative data. Similar SERS analyses were performed for the wear tracks on each a-C:H surface. The measurement depth from the topmost surface was assumed to be important, because the hydrogen concentration decreased from the surface to the interface, as shown in Fig. 3.5.

The depth of the measurement position from the surface was confirmed by using a laser microscope to obtain cross-sectional information, which is summarized in Table 1. All measurement depths from the topmost surfaces were less than 50 nm, so the

hydrogen concentrations were assumed all to be around 30–35 at.% from Fig. 3.5. The G-peak position shifts and I_D/I_G ratios are shown in Figs. 3.13 (a) and (b) for several friction conditions.

Table 3.1: The SERS measurement depth from each a-C:H surface.

Particles in the lubricant	Wear depth from surface h, nm
MoS_2	17
MoDTC	21
Mo	23
Mo_2C	33
MoO_3+Mo	35
MoO_3	37
Mo_2C+MoO_3+Mo	41

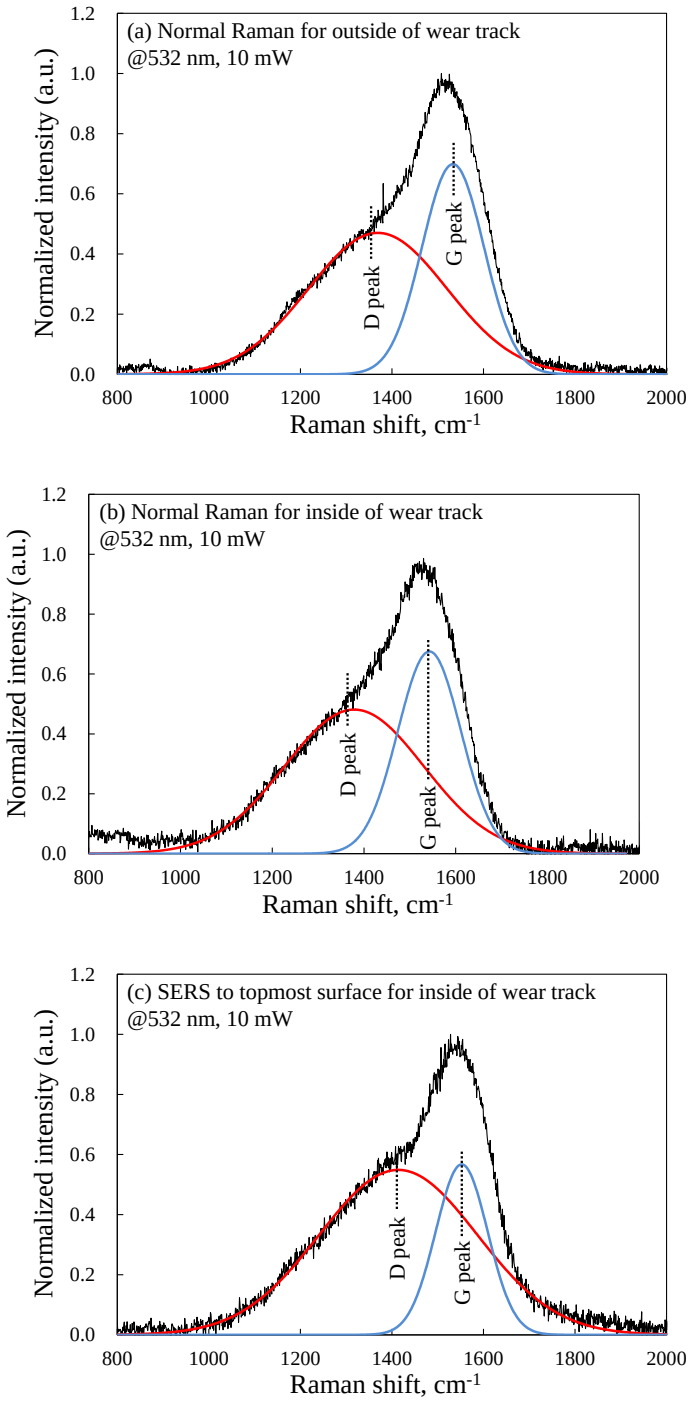

Figure 3.11 The Raman and SERS spectra for a-C:H surfaces. (a) The as-deposited surface (i.e., outside the wear track) from normal Raman analysis. (b) The inside of the wear track from normal Raman analysis. (c) SERS analysis for the inside of the wear track

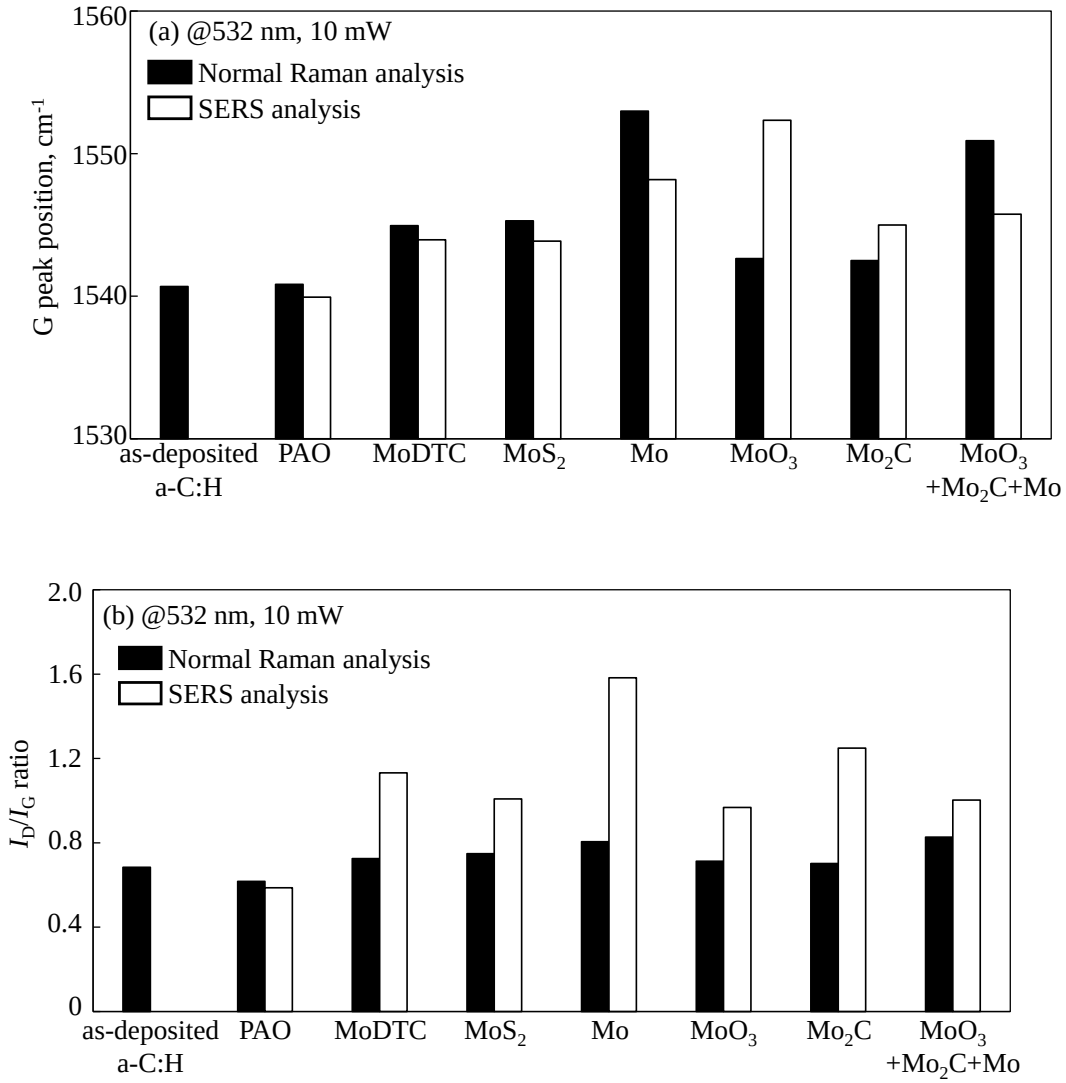

Figure 3.12 Summary of normal Raman and SERS analyses for the a-C:H surfaces. (a) The G-peak position and (b) the ID/IG ratio. The black bars show the normal Raman results, and the white bars show the SERS analysis results

The I_D/I_G ratio shown in Fig. 3.12 (a) indicates that every surface showed a G-peak position shift toward a higher frequency than obtained for the as-deposited surface. The SERS analysis, which provides more information about the topmost surface as compared to normal Raman analysis, shows that MoO_3 had the highest G-peak position among all the specimens, at 1552 cm^{-1}. The I_D/I_G ratio shown in Fig. 3.12 (b) exhibited

little variation among all the specimens measured using normal Raman analysis. The SERS results differed significantly from the normal Raman data, with Mo showing the highest I_D/I_G ratio among all the specimens.

3.4 Discussion

The Raman data from less than 2 nm depth in the topmost surface was obtained by SERS analysis, as reported in our previous study [88]. To compare standard Raman data, which actually represents "bulk" data, and the data from the topmost surface of the wear track, a-C:H disc surfaces resulting from lubrication containing several different types of particles were prepared and analyzed.

The specific wear rate as a function of the hydrogen concentration exhibits several different friction regimes, as shown in Fig. 3.13. The black symbols show the SERS results, which represent surface information only, as compared to the normal Raman spectra shown by the open symbols in the figure. The most interesting point is that among Mo-related powders, only MoS_2 showed a great reduction in the hydrogen content, up to approximately 20 at.%, as observed from the SERS analysis.

This result implies that hydrogen is extracted by MoS_2 powder under boundary lubrication conditions. MoS_2 is a catalyst that can form covalent bonds between sulphur and hydrogen [110], so that hydrogen included in a-C:H surface can be extracted. From the viewpoint of thermal stability of a-C:H coating under 80°C, there was no clear structural change by heating which was shown in Fig. 3.12 (b), such as I_D/I_G ratio under PAO situation.

A previous study reported in the literature [111] showed no clear hardness reduction by applying annealing under 100°C for a-C:H coating, therefore, the hardness of a-C:H coating in this study was assumed to not change during friction tests. On the other hand, braking of chemical bonds between C-H, C-C or other binding was also obtained by applying UV irradiation in several works of literature by presented authors [112-118] and element diffusion to a-C:H coating during friction [119-121].

That structural change was assumed to be taken place as chemical structural change by catalytic effect. So, the specific wear rate in this study as shown in Fig. 3.8 indicated that MoO_3 had the catalytic effect on enhancing specific wear rate under 80°C. The effect of temperature on specific wear rate is summarized in Fig. 3.14 as an Arrhenius plot consisting of a natural logarithm of specific wear rate as a function of an inverse of temperature. Each slope value listed in Table 2 indicated chemical reaction sensitivity so that Mo, MoO_3, and MoS_2 had higher slope values than Mo_2C and MoDTC. This comparison indicated that Mo, MoO_3, and MoS_2 accelerated chemical wear.

Without MoS_2, the other friction test surfaces showed higher hydrogen concentrations from the SERS data, as compared to normal Raman data. These results imply that carbon atoms have been extracted by those particles. From the surface roughness shown in Fig. 3.10, Mo_2C and MoO_3+Mo_2C+Mo showed several scratch marks on the wear tracks. Therefore those two cases were identified as belonging to a separate abrasive-wear regime. For Mo and MoDTC, the surface roughness of the a-C:H coating did not change. The hardness of all powders without Mo_2C is smaller than the a-C:H coating. Thus, the wear acceleration was assumed to be caused by the catalytic effect to compare with the PAO situation.

Some possible wear mechanisms have been summarized in the literature [122], with or without hydrogen in diamond-like carbon was attacked by MoO_3 or Mo-carbides which were generated from the degradation of MoDTC. The degradation of MoDTC was specifically reported by Barros'Bouchet et al., which showed that MoS_2 and MoO_3 were generated under an a-C:H-coated cylinder sliding against an a-C:H-coated AISI 52100 disc under a lubricant containing MoDTC 100˚C [119].

This work showed that MoDTC is first degraded to MoS_2 and that MoO_3 is generated subsequently. The MoS_2 had the possibility of extracting hydrogen from the topmost surface. After several friction cycles from the beginning to the middle of the tests, the a-C:H surface may contain less hydrogen, and then MoO_3 can easily undergo tribo-chemical reactions with carbon atoms.

Finally, Mo_2C generated and dispersed in the lubricant caused a much higher rate of wear by scratches than either MoS_2 or MoO_3 reacting with a-C:H. These assumptions are pictorially summarized in Fig. 3.15.

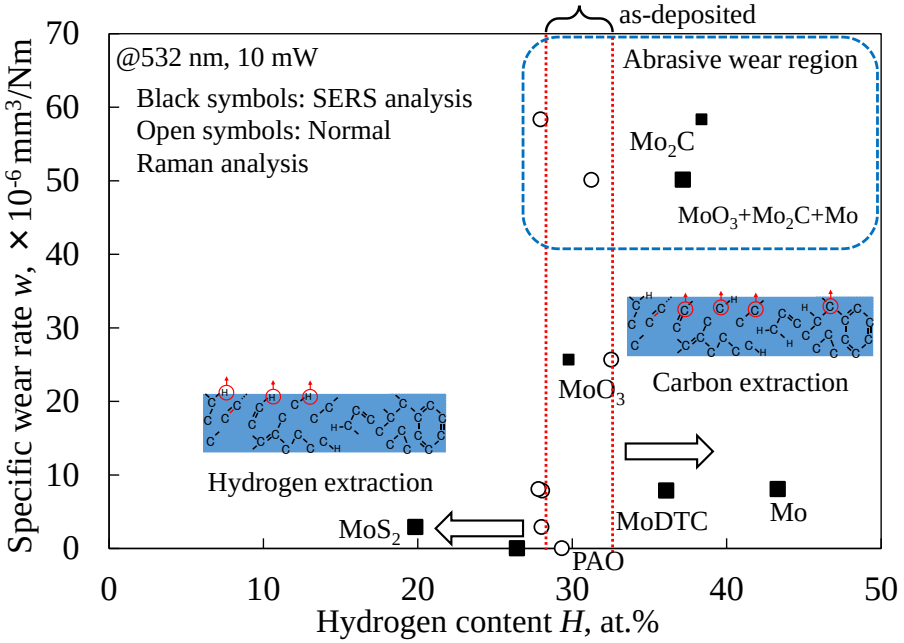

Figure 3.13 The hydrogen concentration for wear tracks in a-C:H coatings, as measured using normal Raman spectra (open symbols) and SERS (black symbols) for different particles

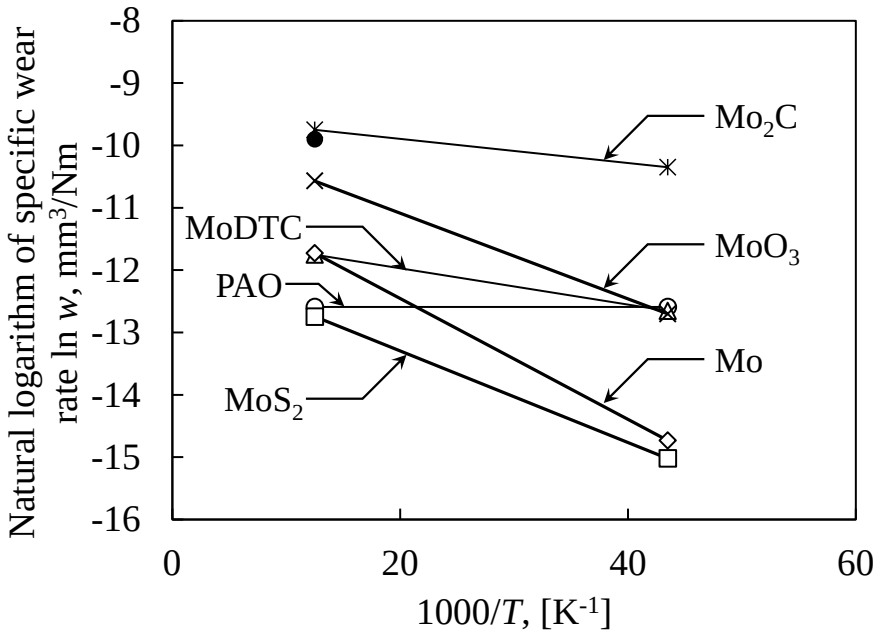

Figure 3.14 The relation between natural logarithm of specific wear rate of a-C:H coating and inverse temperature as Arrhenius plot

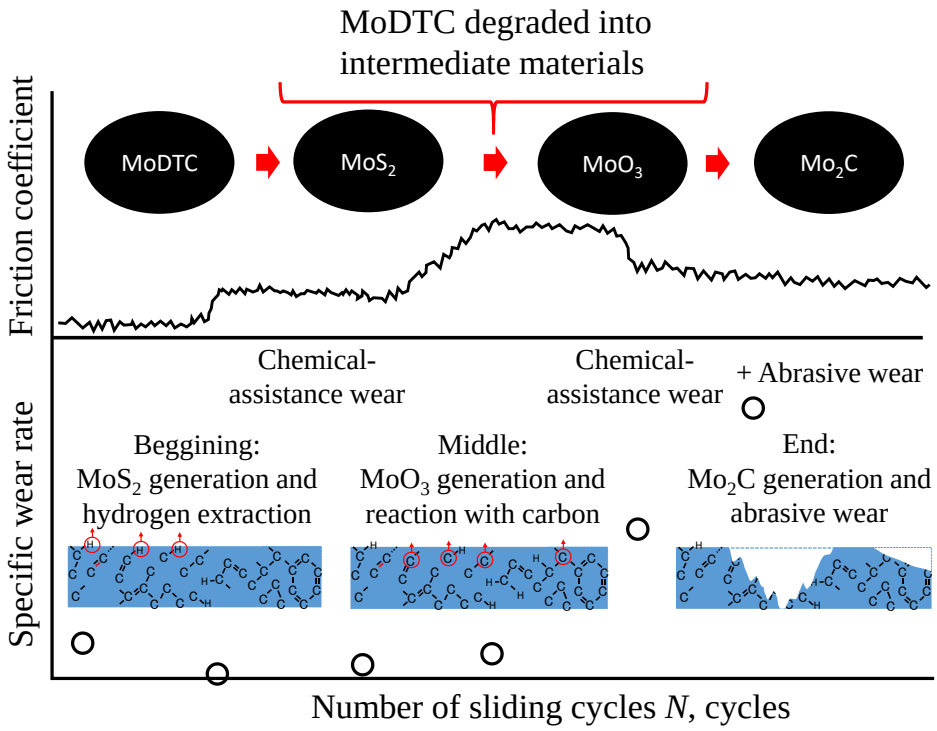

Figure 3.15 Illustration of possible wear acceleration of an a-C:H coating by Mo-related materials

Table 3.2: The summary of the Arrhenius plot slopes of specific wear rate according to each particles

Particle materials & PAO	PAO	MoDTC	MoS_2	Mo	MoO_3	Mo_2C
Effective hardness, GPa	-	1.0	1.0	1.5	2.5	15
Arrhenius plot slope	>-0.001	-0.029	-0.074	-0.097	-0.069	-0.019

3.5 Conclusion

This study investigated the friction and wear of a-C:H coatings against a SUJ2 ball under lubrication with Mo-derived PAO under boundary lubrication at 80˚C. It is often assumed that MoDTC degrades into other materials, leading to a significant wear acceleration of the coating surface.

Therefore, five different types of Mo-derived particles—MoDTC, MoS_2, MoO_3, Mo_2C, and, Mo were studied to determine which Mo-derived compounds play significant roles in enhancing the wear of a-C:H. From the viewpoint of tribological studies at the standard engine temperature of 80ºC, the conclusions are as follows:

- The specific wear rate of an a-C:H coating under a lubricant containing Mo_2C had the highest value, approximately 58×10^{-6} mm^3/Nm. This value is higher than 23°C (about 34×10^{-6} mm^3/Nm), but the increased temperature did not significantly accelerate the wear of the a-C:H coating. Thus, Mo_2C accelerates the wear abrasively.
- The specific wear rate of an a-C:H coating under a lubricant containing MoO_3 was the moderate value of approximately 25.7×10^{-6} mm^3/Nm. However, this value is eight times larger than the specific wear rate at room temperature. Thus, temperature substantially increased the specific wear rate of MoO_3, regardless of the hardness of these particles.
- The Raman data from less than 2 nm depth within the topmost surface by SERS analysis indicated that only MoS_2 showed a significant reduction of the hydrogen content at the topmost surface of the wear track (hydrogen content decreased from 30–35 at.% to 20 at.% of as-deposited). For lubricants that

included Mo or MoDTC, the surfaces showed higher hydrogen concentrations after the friction test according to the SERS data, as compared to normal Raman spectra. These results imply that carbon atoms are extracted by those particles.

Chapter 4

Conclusion

For the past decades, industrial player especially automobile manufacturers are racing to introduce the latest technologies to their products. Among them is the use of diamond-like carbon (DLC) as a coating material on their engine parts in order to have a smaller and lighter engine, to reduce the energy consumption, and to increase the engine lifespan with a technology that has high resistance towards friction and wear. However, the lubrication which consists lubricant additives increased the wear of DLC coating and affected the engine's performance.

The objectives of this study investigate the friction and wear of the hydrogenated amorphous carbon (a-C:H) DLC and silicon-doped a-C:H (Si-DLC) coatings against SUJ2 ball under PAO lubrication with/without Mo-derived particles under boundary lubrication at room temperature and standard operating engine temperature. It is often assumed that MoDTC, which is a well-known friction modifier, degraded into other materials, and lead to the wear acceleration.

Therefore, five different powder-types Mo-derived particles, MoDTC, MoS_2, MoO_3, Mo_2C, and, Mo were dispersed into PAO base oil and tribologically tested to determine which Mo-derived compound plays significant roles in enhancing the wear of a-C:H. After all, the tribological effect of MoDTC degradation are now well understood.

From the tribological analysis at normal room temperature of 23ºC, it can be concluded as follows:

- The specific wear rate of a-C:H coating was higher than Si-DLC under lubrication of MoDTC in PAO oil. The specific wear rate of a-C:H coating was the highest under Mo_2C lubrication. On the other hand, MoO_3 also showed a greater specific wear rate compared to MoS_2 and Mo which had the lowest specific wear rate. Therefore, Mo_2C from the MoDTC degradation was the major contributor to the wear acceleration under boundary lubrication at room temperature and classified as abrasive wear.

- With regards to the MoO_3 containing lubrication, the high specific wear rate result indicates that MoO_3 have affection to accelerate wear as catalytic effect from the view point of hardness. Since the hardness of MoDTC is 1.0 GPa, it was infeasible for MoDTC particles to abrasively accelerate the wear considering the hardness of a-C:H coating (18 GPa) and Si-DLC (25 GPa) are much higher than that of MoDTC. Thus, it is concluded that MoDTC accelerating the wear of a-C:H through tribo-chemical interaction without mechanical effect which can be simplified as chemical-assist wear.

Succeeding the first objective, the tribological analysis continues executed at the standard engine operating temperature of 80ºC. The implementation of surface-enhanced Raman scattering (SERS) procedure plays a very significant role to procure the most accurate and precise information at the critical topmost surface of the DLC coating. Then, the conclusions can be drawn as follows:

- The specific wear rate of an a-C:H coating under Mo_2C containing lubricant had the highest value and this value is higher compared to 23°C. The increase in temperature promotes higher surface graphitization rates which produce lamellar structure that is easily remove by abrasive action. Thus, Mo_2C accelerates the wear abrasively together with surface graphitization enhance the wear rates.

- The specific wear rate of an a-C:H coating had a moderate value under MoO_3 lubrication, but this value was eight times larger than the specific wear rate at room temperature of 23°C. The increment in temperature provide catalytic effect which substantially increases the specific wear rate of a-C:H coating under MoO_3 lubrication, regardless of its hardness.

- The SERS analysis proves that with the presence of MoS_2 in lubricant, the hydrogen diffused from a-C:H coating promotes chemical wear to DLC.
- For lubricants included with Mo or MoDTC, the carbon atoms were extracted by these particles as a result of catalytic effect.

References

[1] Stachowiak, G. W., & Batchelor, A. W. (2013). Engineering tribology. Butterworth-heinemann.

[2] Callister, W. D., & Rethwisch, D. G. (2018). Materials science and engineering: an introduction (Vol. 9, pp. 96-98). New York: Wiley.

[3] U.S. Department of Energy, Material Science. (1993). DOE Fundamentals Handbook, Volume 1 and 2.

[4] Jahanmir, S. (1998). Tribology issues in machining. Machining Science and Technology, 2(1), 137-154.

[5] Hutchings, I., & Shipway, P. (2017). Tribology: friction and wear of engineering materials. Butterworth-Heinemann.

[6] Zhou, Z. R., & Jin, Z. M. (2015). Biotribology: recent progresses and future perspectives. Biosurface and Biotribology, 1(1), 3-24.

[7] Zhang, S. W. (2013). Green tribology: Fundamentals and future development. Friction, 1(2), 186-194.

[8] Boneh, Y., & Reches, Z. E. (2018). Geotribology-Friction, wear, and lubrication of faults. Tectonophysics, 733, 171-181.

[9] Bhushan, B., Israelachvili, J. N., & Landman, U. (1995). Nanotribology: friction, wear and lubrication at the atomic scale. Nature, 374(6523), 607-616.

[10] Liu, Y., Niu, S., & Wang, Z. L. (2015). Theory of tribotronics. Advanced Electronic Materials, 1(9), 1500124.

[11] Roberts, E. W. (2012). Space tribology: its role in spacecraft mechanisms. Journal of Physics D: Applied Physics, 45(50), 503001.

[12] Meng, Y., Xu, J., Ma, L., Jin, Z., Prakash, B., Ma, T., & Wang, W. (2022). A review of advances in tribology in 2020–2021. Friction, 10(10), 1443-1595.

[13] Bhushan, B. (2000). Tribology: Friction, wear, and lubrication. The Engineering Handbook, 80-120.

[14] Buckley, D. H. (1981). Surface effects in adhesion, friction, wear, and lubrication (Vol. 5). Elsevier.

[15] González-Viñas, W. & Mancini, H.L. (2004). An Introduction to Materials Science. Princeton University Press. ISBN 978-0-691-07097-1.

[16] Kato, K. (2005). Classification of wear mechanisms/models. Wear–materials, mechanisms and practice, 9-20.

[17] Stachowiak, G. W. (Ed.). (2006). Wear: materials, mechanisms and practice..

[18] Varenberg, M. (2013). Towards a unified classification of wear. Friction, 1(4), 333-340.

[19] Islam, S., & Ibrahim, R. N. (2011). Mechanism of abrasive wear in nanomachining. Tribology letters, 42(3), 275-284.

[20] Groche, P., & Nitzsche, G. (2007). Influence of temperature on the initiation of adhesive wear with respect to deep drawing of aluminum-alloys. Journal of materials processing technology, 191(1-3), 314-316.

[21] Groche, P., Nitzsche, G., & Elsen, A. (2008). Adhesive wear in deep drawing of aluminum sheets. CIRP annals, 57(1), 295-298.

[22] Angus, J. C., & Wang, Y. (1991). Diamond-like hydrocarbon and carbon films. In Diamond and Diamond-like Films and Coatings (pp. 173-192). Springer, Boston, MA.

[23] Holmberg, K., Andersson, P., & Erdemir, A. (2012). Global energy consumption due to friction in passenger cars. Tribology international, 47, 221-234.

[24] Zhang, S. (2015). Analysis of phase transitions and crystal structures of novel benzothiophene derivatives. The University of Akron..

[25] http://techon.nikkeibp.co.jp/article/HONSHI_LEAF/20050528/105217/, Online article, Access on April (2019). [in Japanese].

[26] Guy, A.G. (1976). Essentials of Materials Science, McGraw-Hill, Inc., New York, USA,

[27] Bhushan, B. (1999). Principles and Applications of Tribology, John Wiley & Sons, Inc, New York, USA.

[28] Dischler, B. (1987). Bonding and hydrogen incorporation in aC: H studied by infrared spectroscopy. EMRS XVII Proceedings; Koidl, P., Oelhafen, P., Eds, 189-201.

[29] Robertson, J. (1992). Mechanical properties and structure of diamond-like carbon. Diamond and Related Materials, 1(5-6), 397-406.

[30] Lam, B.X. (2008). Diamond-like carbon coatings for tribological applications, Sci. Technol. Dev. 11. 100-108.

[31] Ronkainen, H., Varjus, S., Koskinen, J., & Holmberg, K. (2001). Differentiating the tribological performance of hydrogenated and hydrogen-free DLC coatings. Wear, 249(3-4), 260-266.

[32] Koskinen, J., Schneider, D., Ronkainen, H., Muukkonen, T., Varjus, S., Burck, P., & Scheibe, H. J. (1998). Microstructural changes in DLC films due to tribological contact. Surface and Coatings Technology, 108, 385-390.

[33] Robertson, J. (2008). Comparison of diamond-like carbon to diamond for applications. Phys Status Solidi Appl Mater Sci. 205:2233–44.

[34] Overview of Amorphous Carbon Films (2017). doi:10.1007/978-981-10-4882-1.

[35] Zahid, R., Masjuki, H. H., Varman, M., Mufti, R. A., Kalam, M., & Gulzar, M. (2015). Effect of lubricant formulations on the tribological performance of self-mated doped DLC contacts: a review. Tribology Letters, 58(2), 1-28.

[36] Tillmann, W., Vogli, E., & Hoffmann, F. (2009). Wear-resistant and low-friction diamond-like-carbon (DLC)-layers for industrial tribological applications under humid conditions. Surface and Coatings Technology, 204(6-7), 1040-1045.

[37] Sotres, J., & Arnebrant, T. (2013). Experimental investigations of biological lubrication at the nanoscale: the cases of synovial joints and the oral cavity. Lubricants, 1(4), 102-131.

[38] Tung, S. C., & Gao, H. (2003). Tribological characteristics and surface interaction between piston ring coatings and a blend of energy-conserving oils and ethanol fuels. Wear, 255(7-12), 1276-1285.

[39] Tung, S. C., & Gao, H. (2002). Tribological investigation of piston ring coatings operating in an alternative fuel and engine oil blend. Tribology transactions, 45(3), 381-389.

[40] Rejowski, E. D., Mordente, P., PILLIS, M. F., & Casserly, T. (2014). Application of DLC coating in cylinder liners for friction reduction. SAE International.

[41] Mobarak, H. M., Masjuki, H. H., Mohamad, E. N., Rahman, S. A., Al Mahmud, K. A. H., Habibullah, M., & Salauddin, S. (2014). Effect of DLC coating on tribological behavior of cylinder liner-piston ring material combination when lubricated with Jatropha oil. Procedia Engineering, 90, 733-739.

[42] Leslie, R. (2008). Rudnick (Ed.). Lubricant additives: Chemistry and applications. CRS Press, Second Edition.

[43] Morina, A., Neville, A., Priest, M., & Green, J. H. (2006). ZDDP and MoDTC interactions in boundary lubrication—the effect of temperature and ZDDP/MoDTC ratio. Tribology international, 39(12), 1545-1557.

[44] Yue, W., Fu, Z., Wang, S., Gao, X., Huang, H., & Liu, J. (2014). Tribological synergistic effects between plasma nitrided 52100 steel and molybdenum dithiocarbamates additive in boundary lubrication regime. Tribology International, 74, 72-78.

[45] Greenberg, R., Halperin, G., Etsion, I., & Tenne, R. (2004). The effect of WS2 nanoparticles on friction reduction in various lubrication regimes. Tribology Letters, 17(2), 179-186.

[46] de Barros' Bouchet, M. I., Martin, J. M., Le-Mogne, T., & Vacher, B. (2005). Boundary lubrication mechanisms of carbon coatings by MoDTC and ZDDP additives. Tribology International, 38(3), 257-264.

[47] Podgornik, B., Jacobson, S., & Hogmark, S. (2003). DLC coating of boundary lubricated components—advantages of coating one of the contact surfaces rather than both or none. Tribology International, 36(11), 843-849.

[48] Neville, A., Morina, A., Haque, T., & Voong, M. (2007). Compatibility between tribological surfaces and lubricant additives—how friction and wear reduction can be controlled by surface/lube synergies. Tribology international, 40(10-12), 1680-1695.

[49] Forsberg, P., Gustavsson, F., Renman, V., Hieke, A., & Jacobson, S. (2013). Performance of DLC coatings in heated commercial engine oils. Wear, 304(1-2), 211-222.

[50] Kalin, M., & Velkavrh, I. (2013). Non-conventional inverse-Stribeck-curve behaviour and other characteristics of DLC coatings in all lubrication regimes. Wear, 297(1-2), 911-918.

[51] Topolovec-Miklozic, K., Lockwood, F., & Spikes, H. (2008). Behaviour of boundary lubricating additives on DLC coatings. Wear, 265(11-12), 1893-1901.

[52] Kalin, M., Kogovšek, J., & Remškar, M. (2013). Nanoparticles as novel lubricating additives in a green, physically based lubrication technology for DLC coatings. Wear, 303(1-2), 480-485.

[53] Kalin, M., Velkavrh, I., Vižintin, J., & Ožbolt, L. (2008). Review of boundary lubrication mechanisms of DLC coatings used in mechanical applications. Meccanica, 43(6), 623-637.

[54] Masripan, N. A. B., Ohara, K., Umehara, N., Kousaka, H., Tokoroyama, T., Inami, S., & Fujita, M. (2013). Hardness effect of DLC on tribological properties for sliding bearing under boundary lubrication condition in additive-free mineral base oil. Tribology International, 65, 265-269.

[55] Vengudusamy, B., Mufti, R. A., Lamb, G. D., Green, J. H., & Spikes, H. A. (2011). Friction properties of DLC/DLC contacts in base oil. Tribology international, 44(7-8), 922-932.

[56] Yue, W., Liu, C., Fu, Z., Wang, C., Huang, H., & Liu, J. (2013). Synergistic effects between sulfurized W-DLC coating and MoDTC lubricating additive for improvement of tribological performance. Tribology International, 62, 117-123.

[57] Kano, M. (2006). Super low friction of DLC applied to engine cam follower lubricated with ester-containing oil. Tribology International, 39(12), 1682-1685.

[58] Vengudusamy, B., Green, J. H., Lamb, G. D., & Spikes, H. A. (2012). Behaviour of MoDTC in DLC/DLC and DLC/steel contacts. Tribology International, 54, 68-76.

[59] Shinyoshi, T., Fuwa, Y., & Ozaki, Y. (2007). Wear analysis of DLC coating in oil containing Mo-DTC (No. 2007-01-1969). SAE Technical Paper.

[60] Vengudusamy, B., Green, J. H., Lamb, G. D., & Spikes, H. A. (2012). Behaviour of MoDTC in DLC/DLC and DLC/steel contacts. Tribology International, 54, 68-76.

[61] Sugimoto, I., Honda, F., & Inoue, K. (2013). Analysis of wear behavior and graphitization of hydrogenated DLC under boundary lubricant with MoDTC. Wear, 305(1-2), 124-128.

[62] Merlo, A. M. (2003). The contribution of surface engineering to the product performance in the automotive industry. Surface and Coatings Technology, 174, 21-26.

[63] Morina, A., Neville, A., Priest, M., & Green, J. H. (2006). ZDDP and MoDTC interactions in boundary lubrication—the effect of temperature and ZDDP/MoDTC ratio. Tribology international, 39(12), 1545-1557.

[64] Kosarieh, S., Morina, A., Lainé, E., Flemming, J., & Neville, A. (2013). The effect of MoDTC-type friction modifier on the wear performance of a hydrogenated DLC coating. Wear, 302(1-2), 890-898.

[65] Deshpande, P., Minfray, C., Dassenoy, F., Le Mogne, T., Jose, D., Cobian, M., & Thiebaut, B. (2018). Tribocatalytic behaviour of a TiO 2 atmospheric plasma spray (APS) coating in the presence of the friction modifier MoDTC: a parametric study. RSC advances, 8(27), 15056-15068.

[66] De Feo, M., Bouchet, M. D. B., Minfray, C., Esnouf, C., Le Mogne, T., Meunier, F., & Martin, J. M. (2017). Formation of interfacial molybdenum carbide for DLC lubricated by MoDTC: Origin of wear mechanism. Wear, 370, 17-28.

[67] Okubo, H., & Sasaki, S. (2017). In situ Raman observation of structural transformation of diamond-like carbon films lubricated with MoDTC solution: Mechanism of wear acceleration of DLC films lubricated with MoDTC solution. Tribology International, 113, 399-410.

[68] Ohara, K., Hanyuda, K., Kawamura, Y., Omura, K., Kameda, I., Umehara, N., & Kousaka, H. (2017). Analysis of wear track on DLC coatings after sliding with MoDTC-containing lubricants. Tribology Online, 12(3), 110-116.

[69] Windom, B. C., Sawyer, W. G., & Hahn, D. W. (2011). A Raman spectroscopic study of MoS2 and MoO3: applications to tribological systems. Tribology Letters, 42(3), 301-310.

[70] Komori, K., & Umehara, N. (2015). Effect of surface morphology of diamond-like carbon coating on friction, wear behavior and tribo-chemical reactions under engine-oil lubricated condition. Tribology International, 84, 100-109.

[71] Komori, K., & Umehara, N. (2017). Friction and wear properties of tetrahedral Si-containing hydrogenated diamond-like carbon coating under lubricated condition with engine-oil containing ZnDTP and MoDTC. Tribology Online, 12(3), 123-134.

[72] Tasdemir, H. A., Wakayama, M., Tokoroyama, T., Kousaka, H., Umehara, N., Mabuchi, Y., & Higuchi, T. (2013). Ultra-low friction of tetrahedral amorphous diamond-like carbon (ta-C DLC) under boundary lubrication in poly alpha-olefin (PAO) with additives. Tribology International, 65, 286-294.

[73] Tasdemir, H. A., Wakayama, M., Tokoroyama, T., Kousaka, H., Umehara, N., Mabuchi, Y., & Higuchi, T. (2013). Wear behaviour of tetrahedral amorphous diamond-like carbon (ta-C DLC) in additive containing lubricants. Wear, 307(1-2), 1-9.

[74] Tasdemir, H. A., Wakayama, M., Tokoroyama, T., Kousaka, H., Umehara, N., Mabuchi, Y., & Higuchi, T. (2014). The effect of oil temperature and additive concentration on the wear of non-hydrogenated DLC coating. Tribology International, 77, 65-71.

[75] Tasdemir, H. A., Tokoroyama, T., Kousaka, H., Umehara, N., & Mabuchi, Y. (2014). Influence of zinc dialkyldithiophosphate tribofilm formation on the tribological performance of self-mated diamond-like carbon contacts under boundary lubrication. Thin Solid Films, 562, 389-397.

[76] Tokoroyama, T., Goto, M., Umehara, N., Nakamura, T., & Honda, F. (2006). Effect of nitrogen atoms desorption on the friction of the CNx coating against Si3N4 ball in nitrogen gas. Tribology letters, 22(3), 215-220.

[77] Haque, T., Morina, A., Neville, A., Kapadia, R., & Arrowsmith, S. (2009). Effect of oil additives on the durability of hydrogenated DLC coating under boundary lubrication conditions. Wear, 266(1-2), 147-157.

[78] Spikes, H. (2004). The history and mechanisms of ZDDP. Tribology letters, 17(3), 469-489.

[79] Héau, C., Ould, C., & Maurin-Perrier, P. (2013). Tribological behaviour analysis of hydrogenated and nonhydrogenated DLC lubricated by oils with and without additives. Lubrication Science, 25(4), 275-285.

[80] Yang, L., Neville, A., Brown, A., Ransom, P., & Morina, A. (2014). Friction reduction mechanisms in boundary lubricated W-doped DLC coatings. Tribology International, 70, 26-33.

[81] Bouchet, M. D. B., Martin, J. M., Le Mogne, T., Bilas, P., Vacher, B., & Yamada, Y. (2005). Mechanisms of MoS2 formation by MoDTC in presence of ZnDTP: effect of oxidative degradation. Wear, 258(11-12), 1643-1650.

[82] Masuko, M., Ono, T., Aoki, S., Suzuki, A., & Ito, H. (2015). Friction and wear characteristics of DLC coatings with different hydrogen content lubricated with several Mo-containing compounds and their related compounds. Tribology International, 82, 350-357.

[83] Yue, W., Liu, C., Fu, Z., Wang, C., Huang, H., & Liu, J. (2014). Effects of molybdenum dithiocarbamate and zinc dialkyl dithiophosphate additives on tribological behaviors of hydrogenated diamond-like carbon coatings. Materials & Design, 64, 601-607.

[84] Onodera, T., Morita, Y., Suzuki, A., Sahnoun, R., Koyama, M., Tsuboi, H., & Miyamoto, A. (2008). A theoretical investigation on the dynamic behavior of molybdenum dithiocarbamate molecule in the engine oil phase. Tribology Online, 3(2), 80-85.

[85] Sugimoto, I., Honda, F., & Inoue, K. (2013). Analysis of wear behavior and graphitization of hydrogenated DLC under boundary lubricant with MoDTC. Wear, 305(1-2), 124-128.

[86] Ferrari, A. C., & Robertson, J. (2000). Interpretation of Raman spectra of disordered and amorphous carbon. Physical review B, 61(20), 14095.

[87] Harima, H. (2008). UV-Raman observation of Si surface layer with very shallow ion implantation. Kenbikyo, vol. 43, no. 2, pp. 133–136.

[88] Tokoroyama, T., Murashima, M., & Umehara, N. (2020). The surface enhanced raman scattering analysis for carbonaceous coating by using Au nano-particles. Tribology Online, 15(5), 300-308.

[89] Tokoroyama, T., & Umehara, N. (2022). The wear acceleration of aC: H coating by Mo-derived particles under 80ºC temperature. In Proceedings of SAKURA Symposium on Surface Technology and Engineering Materials 2022 (Vol. 2022, pp. 18-19). Malaysian Tribology Society.

[90] Willets, K. A., & Van Duyne, R. P. (2007). Localized surface plasmon resonance spectroscopy and sensing. Annual review of physical chemistry, 58(1), 267-297.

[91] Félidj, N., Aubard, J., Lévi, G., Krenn, J. R., Hohenau, A., Schider, G., & Aussenegg, F. R. (2003). Optimized surface-enhanced Raman scattering on gold nanoparticle arrays. Applied Physics Letters, 82(18), 3095-3097.

[92] Ye, J., Bonroy, K., Nelis, D., Frederix, F., D'Haen, J., Maes, G., & Borghs, G. (2008). Enhanced localized surface plasmon resonance sensing on three-dimensional gold nanoparticles assemblies. Colloids and Surfaces A: Physicochemical and Engineering Aspects, 321(1-3), 313-317.

[93] Toderas, F., Baia, M., Baia, L., & Astilean, S. (2007). Controlling gold nanoparticle assemblies for efficient surface-enhanced Raman scattering and localized surface plasmon resonance sensors. Nanotechnology, 18(25), 255702.

[94] Feng, S., Zheng, Z., Xu, Y., Lin, J., Chen, G., Weng, C., & Zeng, H. (2017). A noninvasive cancer detection strategy based on gold nanoparticle surface-enhanced raman spectroscopy of urinary modified nucleosides isolated by affinity chromatography. Biosensors and Bioelectronics, 91, 616-622.

[95] Donnet, C., & Erdemir, A. (Eds.). (2007). Tribology of diamond-like carbon films: fundamentals and applications. Springer Science & Business Media.

[96] Sharma, R., Barhai, P. K., & Kumari, N. (2008). Corrosion resistant behaviour of DLC films. Thin Solid Films, 516(16), 5397-5403.

[97] Lam, B. X. (2008). DIAMOND-LIKE CARBON COATINGS FOR TRIBOLOGICAL APPLICATIONS. Science and Technology Development Journal, 11(10), 100-109.

[98] Mutyala, K. C., Singh, H., Fouts, J. A., Evans, R. D., & Doll, G. L. (2016). Influence of MoS2 on the rolling contact performance of bearing steels in boundary lubrication: a different approach. Tribology Letters, 61(2), 1-11.

[99] International Energy Agency. Energy Technol Perspect 2012:445.

[100] Mihara, Y. (2017). Research trend of friction loss reduction in internal combustion engines. Tribology Online, 12(3), 82-88.

[101] Tokoroyama, T., Kamiya, T., Afmad, N. A. B. H., & Umehara, N. (2018). Collecting micrometer-sized wear particles generated between DLC/DLC surfaces under boundary lubrication with an electric field. Mechanical Engineering Letters, 4, 18-00089.

[102] Ohara K, Tokoroyama T, Kousaka H, Umehara N. (2014). Analysis method of wear particles from DLC sliding against itself under oil lubrication. Japanese Soc Tribol, 59: 429–36 [in Japanese].

[103] Tokoroyama, T., Kaneko, T., Tsukiyama, Y., Umehara, N., Sato, T., & Suzuki, T. (2013). Effect of texturing on friction properties of CNx coating layer under oil lubrication with imitation wear debris. Trans. Jpn. Soc. Mech. Eng. C, 79(806), 3895-3903.

[104] Kassim, K. A. M., Tokoroyama, T., Murashima, M., & Umehara, N. (2020). The wear classification of MoDTC-derived particles on silicon and hydrogenated diamond-like carbon at room temperature. Tribology International, 147, 106176.

[105] Al-Jeboori, Y., Kosarieh, S., Morina, A., & Neville, A. (2018). Investigation of pure sliding and sliding/rolling contacts in a DLC/Cast iron system when lubricated in oils containing MoDTC-Type friction modifier. Tribology International, 122, 23-37.

[106] Espejo, C., Thiébaut, B., Jarnias, F., Wang, C., Neville, A., & Morina, A. (2019). MoDTC tribochemistry in steel/steel and steel/diamond-like-carbon systems lubricated with model lubricants and fully formulated engine oils. Journal of Tribology, 141(1), 012301.

[107] Okubo, H., Sasaki, S., Lancon, D., Jarnias, F., & Thiébaut, B. (2020). Tribo-Raman-SLIM observation for diamond-like carbon lubricated with fully formulated oils with different wear levels at DLC/steel contacts. Wear, 454, 203326.

[108] Aboua, K. A. M., Umehara, N., Kousaka, H., Tokoroyama, T., Murashima, M., Tasdemir, H. A., & Higuchi, T. (2018). Effect of ZnDTP triboflim's morphology on friction behaviors of DLC coatings: Tribofilm characterization by 3D scanning electron microscope observation. Journal of Advanced Mechanical Design, Systems, and Manufacturing, 12(7), JAMDSM0129-JAMDSM0129.

[109] Casiraghi, C., Piazza, F., Ferrari, A. C., Grambole, D., & Robertson, J. (2005). Bonding in hydrogenated diamond-like carbon by Raman spectroscopy. Diamond and Related Materials, 14(3-7), 1098-1102.

[110] Hinnemann, B., Moses, P. G., Bonde, J., Jørgensen, K. P., Nielsen, J. H., Horch, S., & Nørskov, J. K. (2005). Biomimetic hydrogen evolution: MoS2 nanoparticles as catalyst for hydrogen evolution. Journal of the American Chemical Society, 127(15), 5308-5309.

[111] Deng, X., Kousaka, H., Tokoroyama, T., & Umehara, N. (2013). Thermal stability and high-temperature tribological properties of aC: H and Si-DLC deposited by microwave sheath voltage combination plasma. Tribology Online, 8(4), 257-264.

[112] Tokoroyama, T., Goto, M., Umehara, N., Nakamura, T., & Honda, F. (2006). Effect of nitrogen atoms desorption on the friction of the CNx coating against Si3N4 ball in nitrogen gas. Tribology letters, 22(3), 215-220.

[113] Tokoroyama, T., Kamiya, M., Umehara, N., Wang, C., & Diao, D. (2012). Influence of UV irradiation in low frictional performance of CNx coatings. Lubrication Science, 24(3), 129-139.

[114] Tokoroyama, T., Kamiya, M., Umehara, N., & Fuwa, Y. (2010). The Effect of Ultraviolet Ray Irradiation on Tribological Property of Carbon Nitride Coating. Journal of Japanese Society of Tribologists, 55(9).

[115] Tokoroyama T, Hatano T, Umehara N, Fuwa Y. (2010). The effect of ultraviolet irradiation on friction coefficient of diamond-like carbon coating in air. Trans Japanese Soc Mech Eng, 76: 3166–71 [in Japanese].

[116] Tokoroyama, T., Umehara, N., Hatano, T., & Fuwa, Y. (2011). The Effect of Ultraviolet Light Irradiation on Friction Coefficient of Diamond-Like Carbon Coating under Lubrication. Journal of Japanese Society of Tribologists, 56(4), 256-263.

[117] bin Taib, M. T., Umehara, N., Tokoroyama, T., & Murashima, M. (2018). The effect of UV irradiation to aC: H on friction and wear properties under PAO oil lubrication including MoDTC and ZnDTP. Tribology Online, 13(3), 119-130.

[118] bin Taib, M. T., Umehara, N., Tokoroyama, T., Murashima, M., & Tunggal, D. (2018). The effects of oil additives and mating materials to the friction, wear and seizure characteristics of aC: H coating. Jurnal Tribologi, 18, 1-19.

[119] Aboua, K. A. M., Umehara, N., Kousaka, H., Tokoroyama, T., Murashima, M., Mabuchi, Y., & Kawaguchi, M. (2018). Effect of carbon diffusion on friction and wear behaviors of diamond-like carbon coating against Cr-plating in boundary base oil lubrication. Tribology Online, 13(5), 290-300.

[120] Aboua, K. A. M., Umehara, N., Kousaka, H., Tokoroyama, T., Murashima, M., Mabuchi, Y., & Kawaguchi, M. (2019). Effect of carbon diffusion on friction and wear behaviors of diamond-like carbon coating against germanium in boundary base oil lubrication. Tribology Letters, 67(2), 1-11.

[121] Aboua, K. A. M., Umehara, N., Kousaka, H., Tokoroyama, T., Murashima, M., Mustafa, M. M. B., & Kawaguchi, M. (2020). Effect of mating material and graphitization on wear of aC: H coating in boundary base oil lubrication. Tribology Letters, 68(1), 1-8.

[122] Yoshida, Y., & Kunitsugu, S. (2018). Friction wear characteristics of diamond-like carbon coatings in oils containing molybdenum dialkyldithiocarbamate additive. Wear, 414, 118-125.

Publication List

International Journals:

- **Kassim K.A.M.**, Tokoroyama T, Murashima M, Umehara N. The Wear Classification of Molybdenum-derived Particles on Silicon and Hydrogenated Diamond-Like Carbon at Room Temperature. Tribology International 2020; 147: 106176.
- **Kassim, K. A. M.,** Tokoroyama, T., Murashima, M., Lee, W. Y., Umehara, N., & Mustafa, M. M. B. Wear acceleration of a-C:H coatings by Molybdenum-derived particles: Mixing and temperature effects. Tribology International 2021; 106944.

International Conferences:

- **Kassim K.A.M.**, Tokoroyama T, Murashima M, Umehara N. The Effect of Molybdenum Carbide (Mo_2C) Particles on Wear Properties of Diamond-like Carbon under Boundary Lubrication. The 6th Asia International Conference on Tribology (ASIATRIB), Sarawak (Malaysia), Sept., 2018.
- **Kassim K.A.M.**, Tokoroyama T, Murashima M, Umehara N. The Wear Effect of Molybdenum-derived Particles on Hydrogenated Amorphous DLC at High Temperature. The 8^{th} International Conference on Mechanics and Materials in Design (M2D), Bologna (Italy), Sept., 2019.
- **Kassim K.A.M.**, Tokoroyama T, Murashima M, Umehara N. The Wear Acceleration of a-C:H DLC by Molybdenum-derived Mixed Particles. The International Tribology Conference (ITC), Sendai (Japan), Sept., 2019.